Arab Academy
for Science , Technology and Maritime Transport

13 Marlog 2024

The International Maritime Transport and Logistics Conference

"MARLOG 13"

Towards Smart Green Blue Infrastructure

3-5 March 2024 - Alexandria, Egypt

Eng. Ahmed Abdallah

Elevating Wind Energy Harvesting with J-shaped Blades: A CFD-driven Analysis of H-Darrieus Vertical Axis Wind Turbines

Ahmed Abdallah , Micheal A. William and Iham F. Zidane 3

Outline

1. Background-Motivation
2. Research Objectives
3. Problem describtion and setup
    - *H-Darrieus wind turbine geometry features*
    - *Wind turbine governing parameters*
    - *Numerical details and solver setup*
    - Numerical setup
4. VERIFICATION AND VALIDATION
5. J-BLADE CONFGURATION
6. RESULTS AND DISCUSSION
    - Starting Torque
    - Standard Operational Conditions
7. Conclusions

according to topics

Background Motivation

according to
topics

- Energy shortages and environmental deterioration drive renewable energy demand. Due to technical advances, wind energy has a low environmental effect and low operational costs [1].

- Wind turbines have a either horizontal or vertical axis. Large onshore and offshore projects require HAWTs, whereas suburban areas prefer VAWTs, for which low wind-speed has a large impact on the turbine's performance.

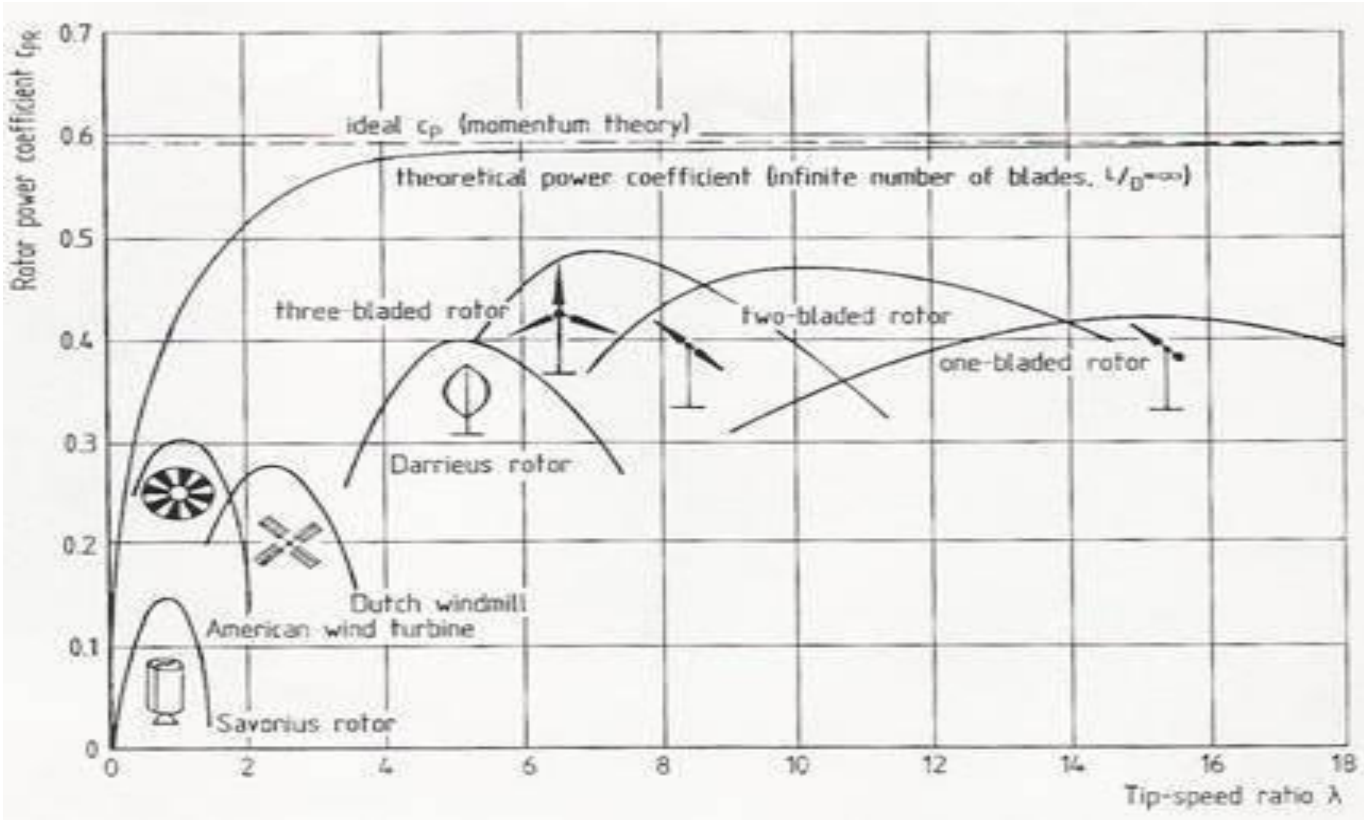

Figure 1. Comparison of turbines performance VS TSR

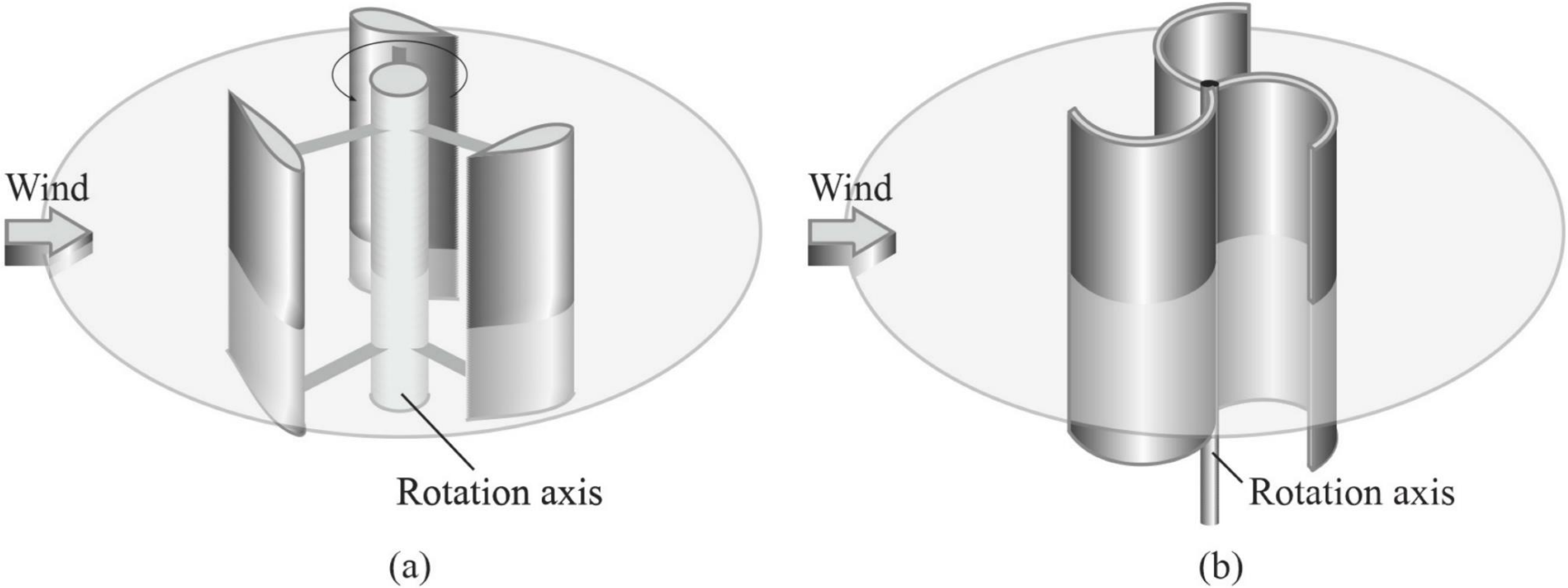

Figure 2. (a) Darrius Turbine; (b) Savanous Turbine

However, other design strategies have been investigated, such as:

- the use of helical blades, or the addition of flaps or vortex generators to the blades [15].
- the use of augmentation technologies on vertical DAWT [4,16].
- Slotted blades have also been investigated recently [17,18].
- Upstream Deflector blades have also been investigated recently [25].
- One innovative idea was through opening the blade trailing edge, and forming what is called a J-shaped blade [19,20].

according to topics

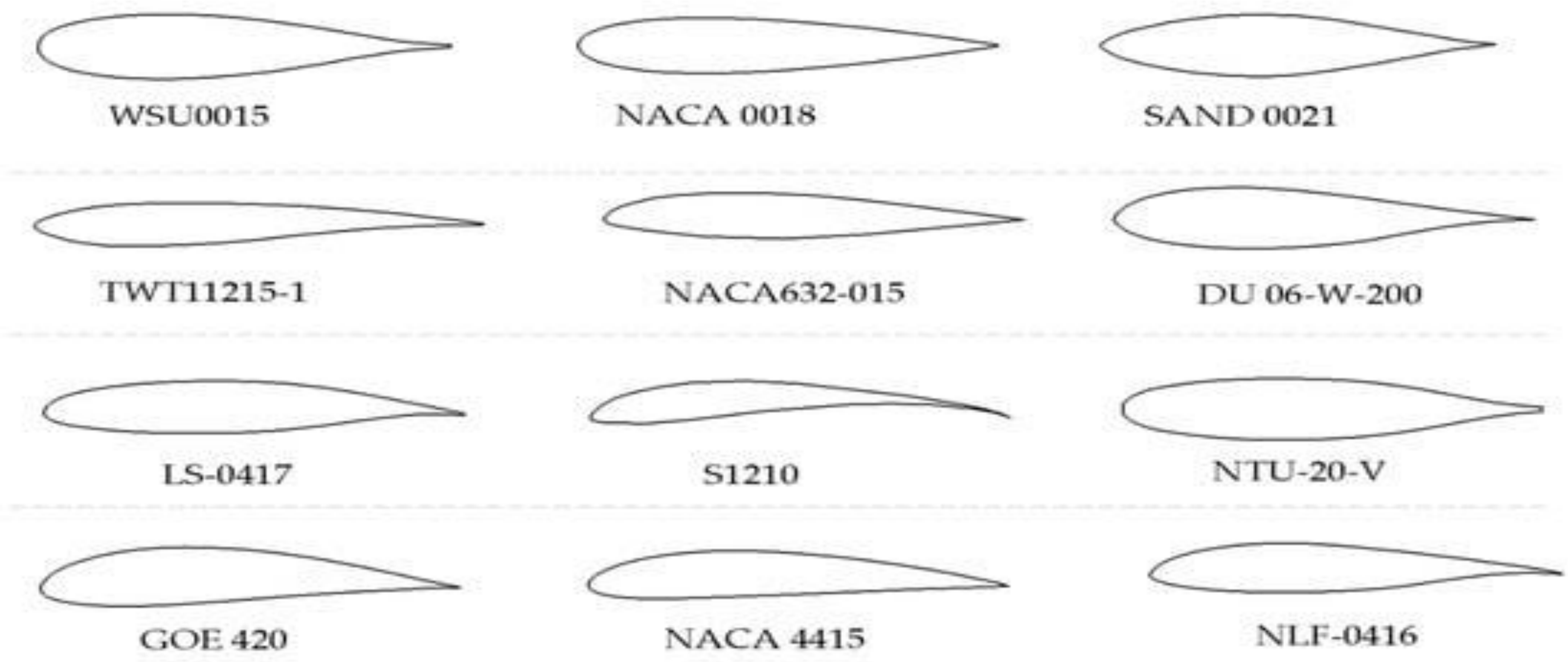

Figure 3. Airfoil Characteristics

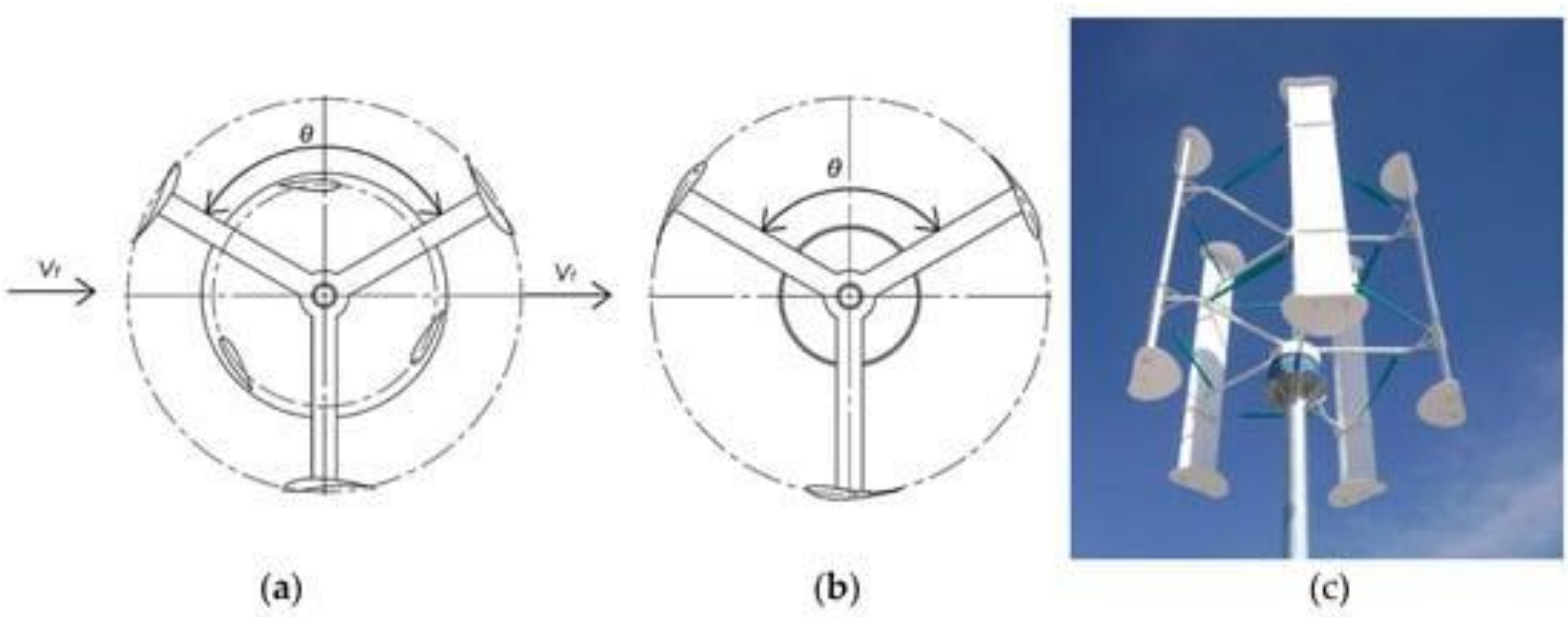

Figure 4. (a) Concave-In; (b) Concave-Out; (c) Turbine with cambered blades.

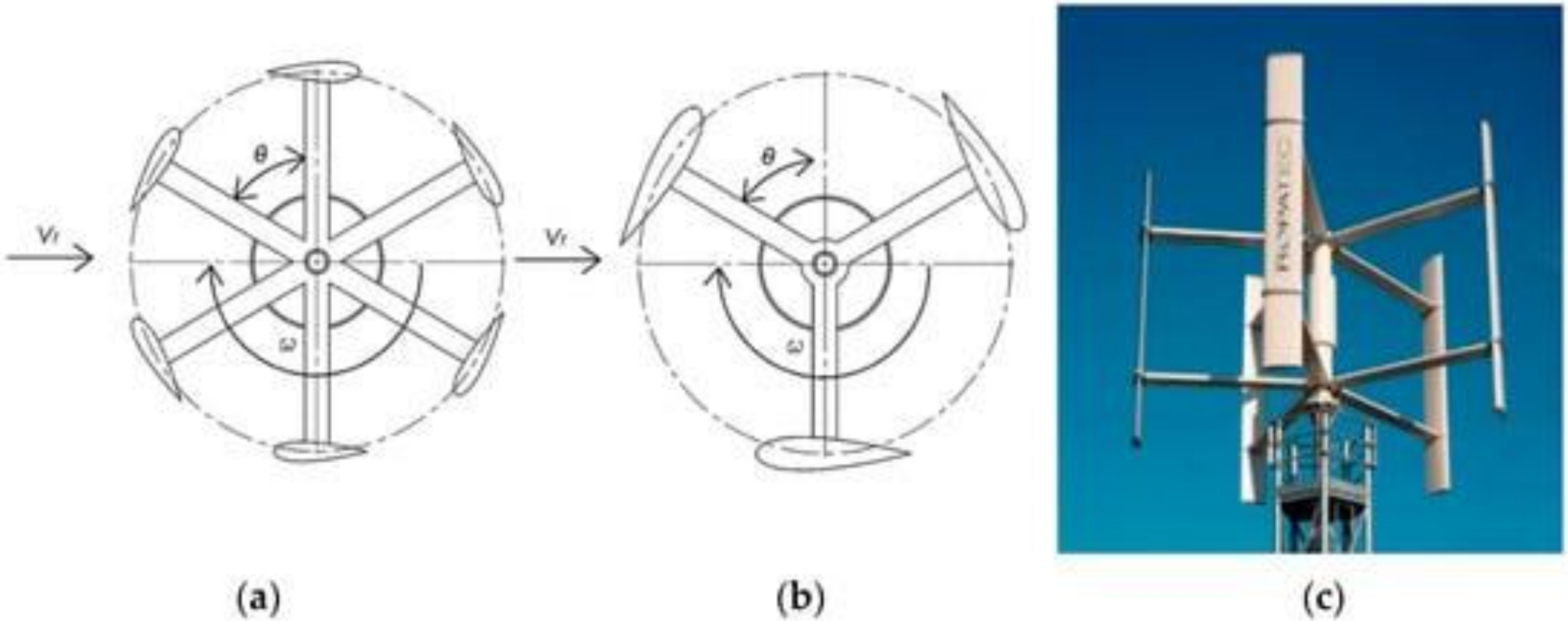

Figure 5. (a) Increased number of blades (b) Increased chord (c) High solidity turbine

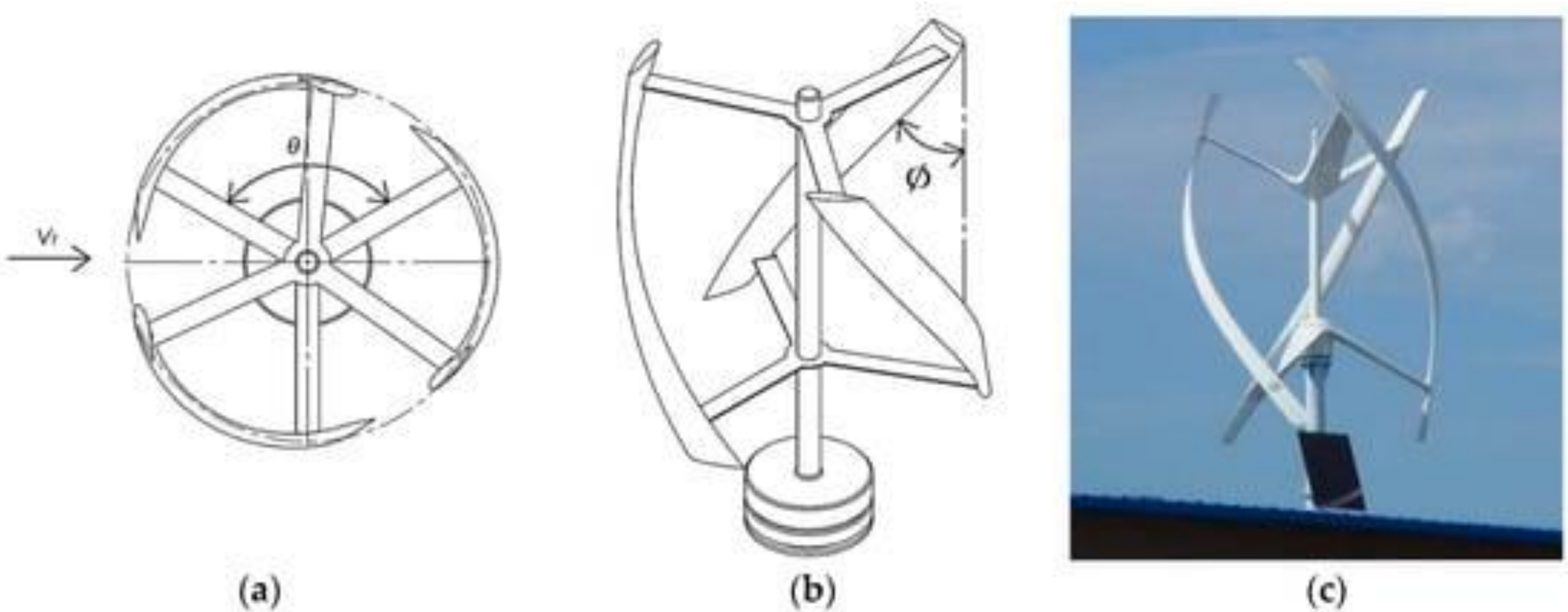

Figure 6. (a) Top view (b) Front view of helical rotor (c) Commercial helical turbine.

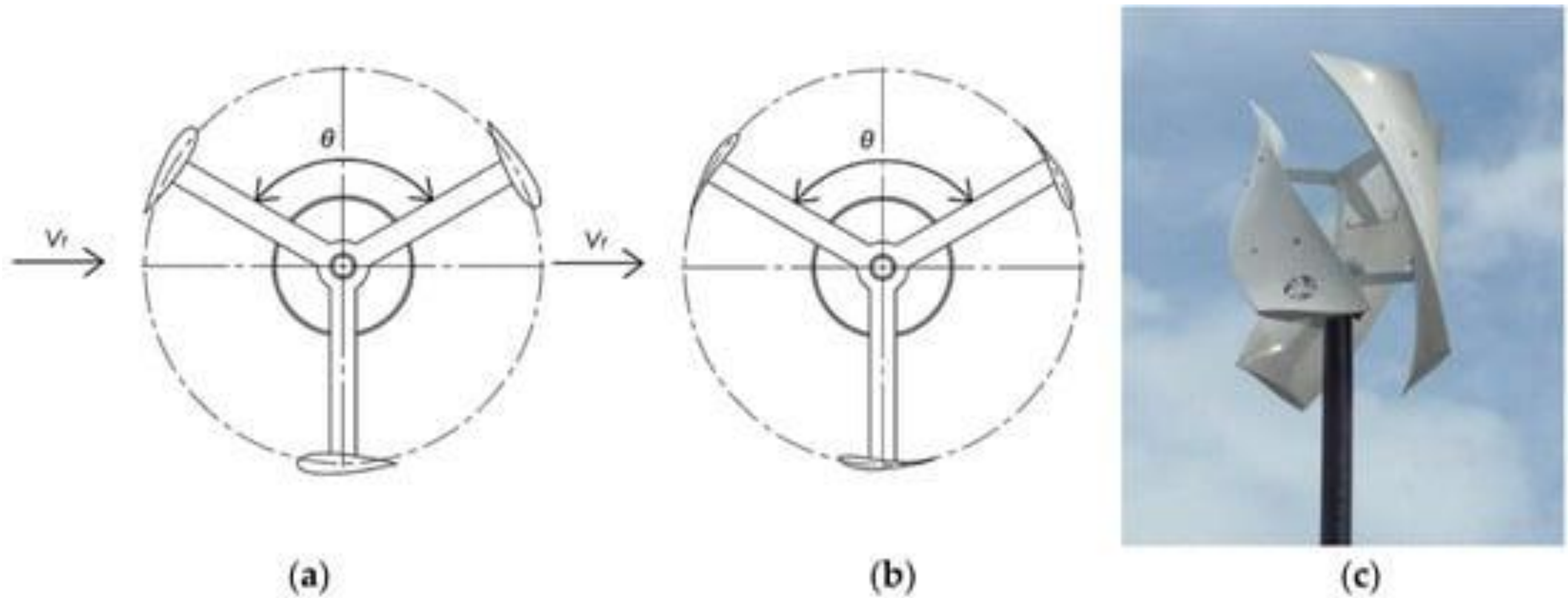

Figure 7. (a) H-Rotor with NACA 0021 (thick) airfoil (b) H-Rotor with S1210 (thin) airfoil (c) Commercial turbine with thicker blade.

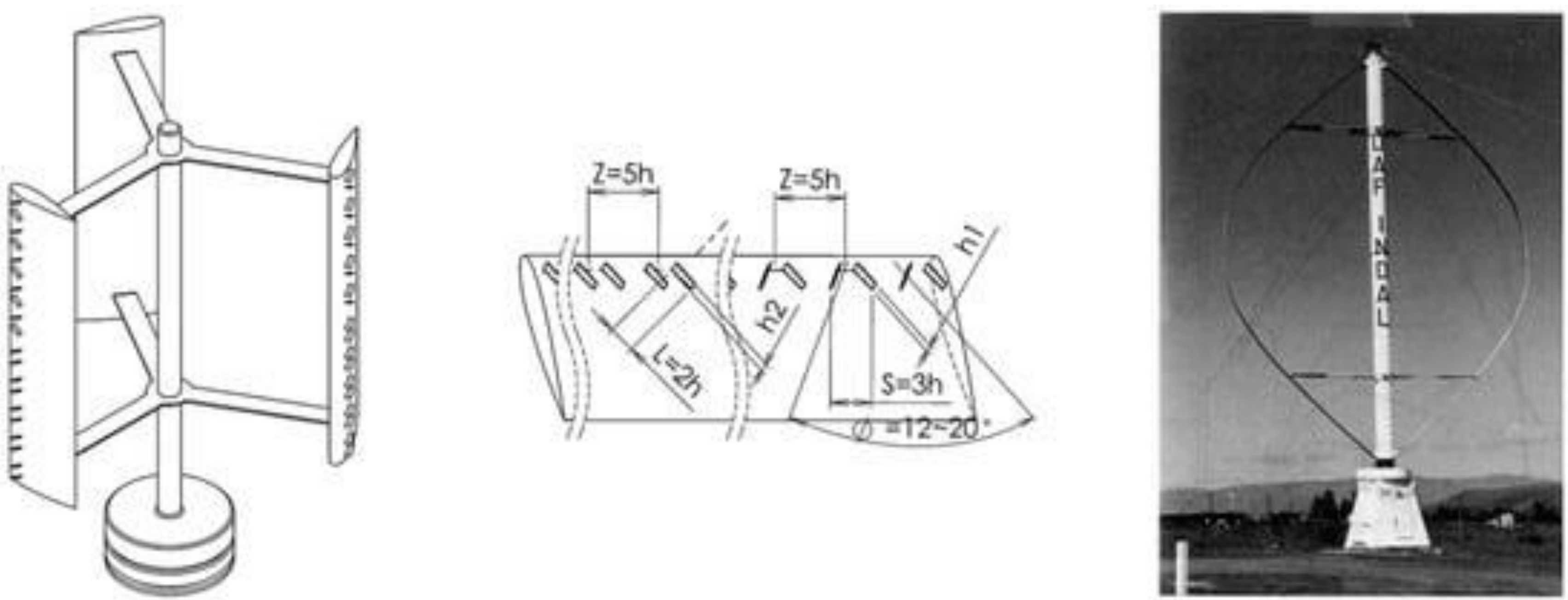

(a) (b) (c)

Figure 8. (a) H-Rotor with VG; (b) Typical VG details; (c) DAF INDAL turbine with VG.

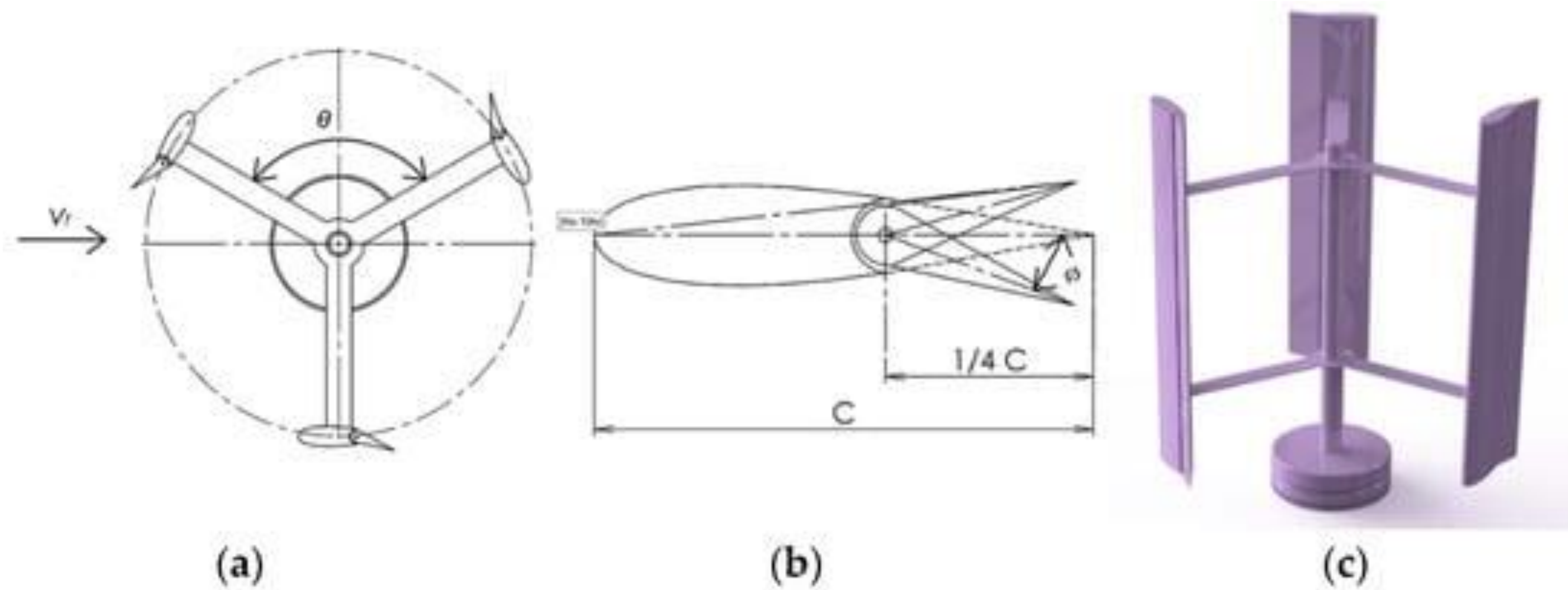

Figure 9. (a) H-rotor with a trailing edge flap (b) Details of an airfoil with a trailing edge flap (c) Illustration of a H-rotor with trailing edge flaps.

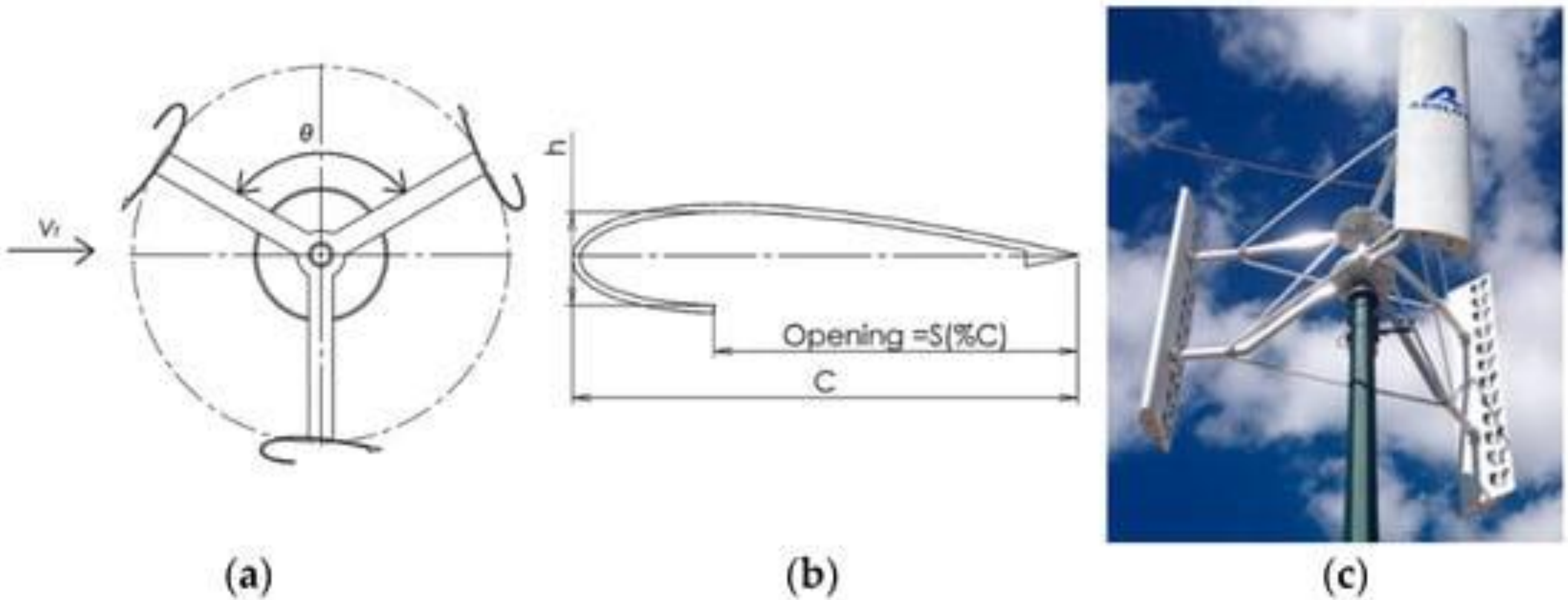

Figure 10. (a) H-Rotor with J-profile airfoil (b) Details of J-profile airfoil (c) Commercial turbine with J-profiled blade.

Table 1. Comparison of strategies, their merits, and demerits.

Strategy	Merits	Demerits
Airfoil characteristics	Less complex, cost-effective, better optimization of dynamic stall, blade tip loss. Increased structural rigidity	Minimal improvement in starting performance and overall power coefficient
Cambered airfoil	Better starting capability delayed stall, less sensitive to surface roughness, high pitching moment	Increased drag on the down half, reduction in power coefficient
Solidity	Increased starting torque, low centrifugal forces due to low rpm	Large AoA, large drive train size and additional cost due to an increased number of blades
Helical blades	Improved aesthetics, smooth torque pulsation leading to reduced vibration	High manufacturing cost of blades, low torque for every azimuthal position
Blade thickness	Better performance at low Re delayed stall and structurally sound	Increased profile drag at high Re and noise
Vortex generators	Improved performance at low Re, extended dynamic stall and marginal improvement in starting torque	Increased drag at high TSR and increases noise due to vortex shedding
Gurney flaps	Delayed dynamic stall with an increase in starting torque compared to a conventional airfoil	Vibration after stall and noise due to vortex shedding
Trailing edge flaps	Better performance in high and low TSR, able to regulate the rotor rpm aerodynamically	Power has to be expended to operate flaps, requires a sophisticated control system
J-Blade	Excellent startup torque, able to sustain low wind speed rotation, ease of blade manufacturing	Degraded performance at high TSR due to high form drag at high Re and increased fatigue failure of blades

- Numerical studies on J-shaped airfoils [19,20] have demonstrated that the self-starting ability of a VAWTs could be improved using an opening on the airfoil. Research indeed showed an almost linear starting torque enhancement with a cut in the outer part of the blade [19].
- Other authors had different views, they claimed that a J-shaped blade design does not provide any performance enhancement [22], and they did not recommend their use for Darrieus-type VAWTs.

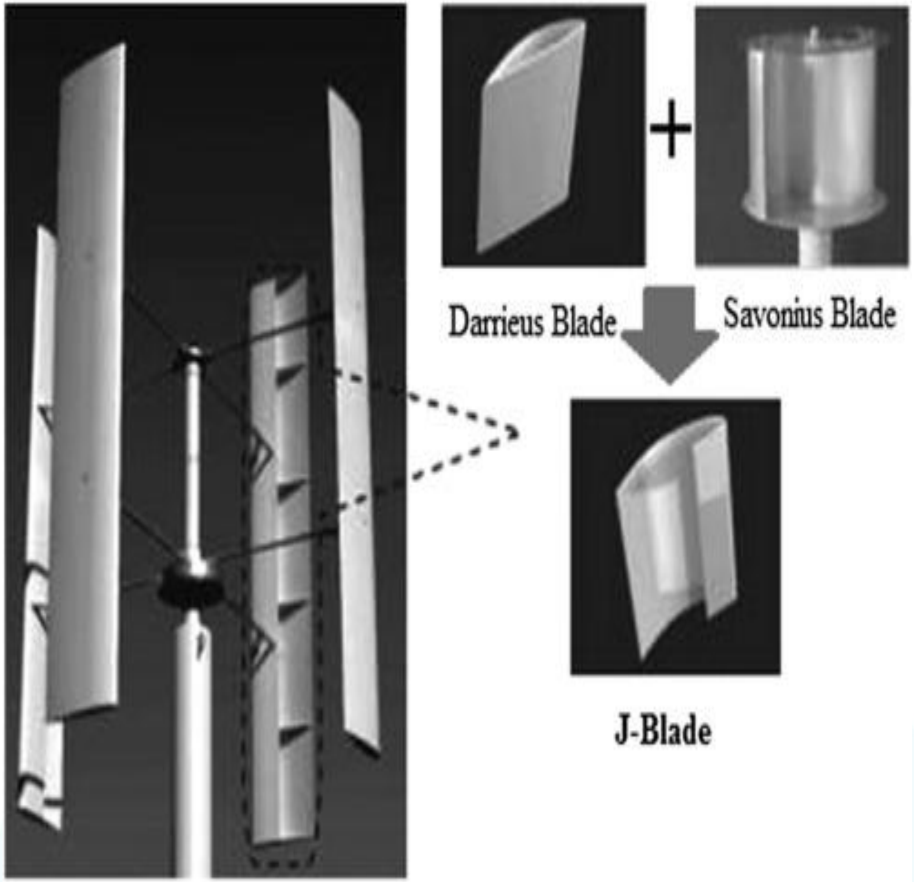

- Further research was performed here to evaluate the effect of the solidity and λ on the performance of Darrieus VAWTs. Two main regions are usually considered for the operational regions of Darrieus turbines, either operating in the high TSR region (λ = 5 or λ = 6) or operating in the low TSR region (λ = 1.5) [23].

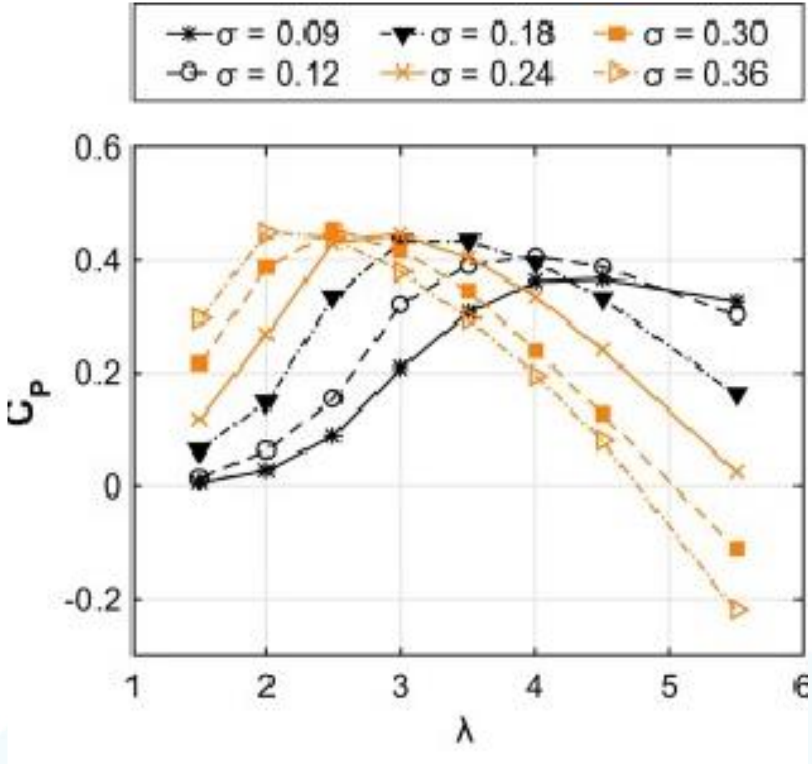

- For high TSR values, the wind flow is mainly attached to the airfoil, due to the low angles of attack. However, when the TSR is in the low region, the angle of attack of the flow on the airfoil increases, leading to dynamic stall effects that highly influence the turbine performance [23]

- **Thus, high solidity (typically around 0.3–0.5) and low TSR seem favorable for the J-shaped design.**

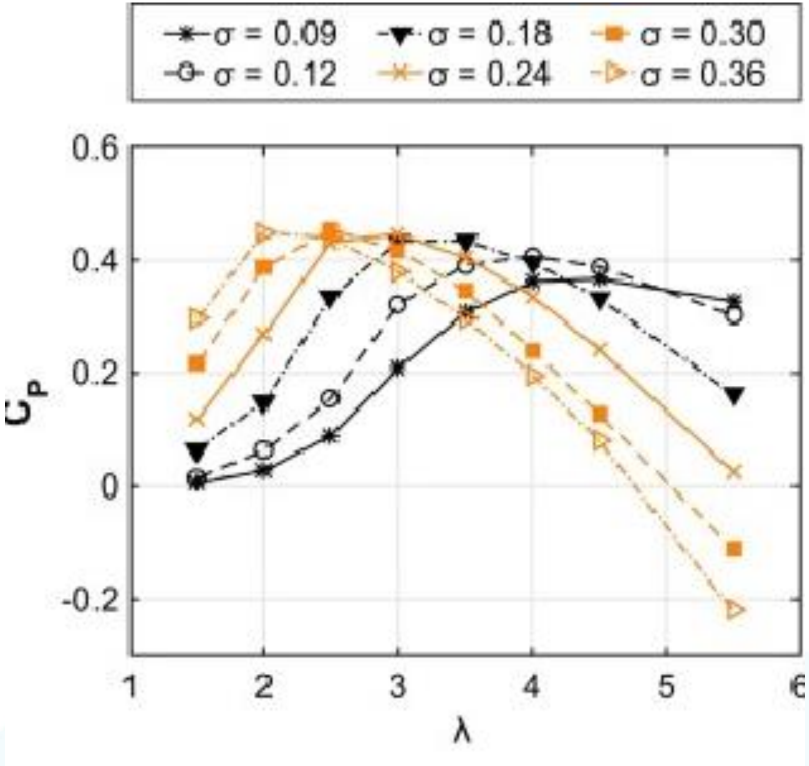

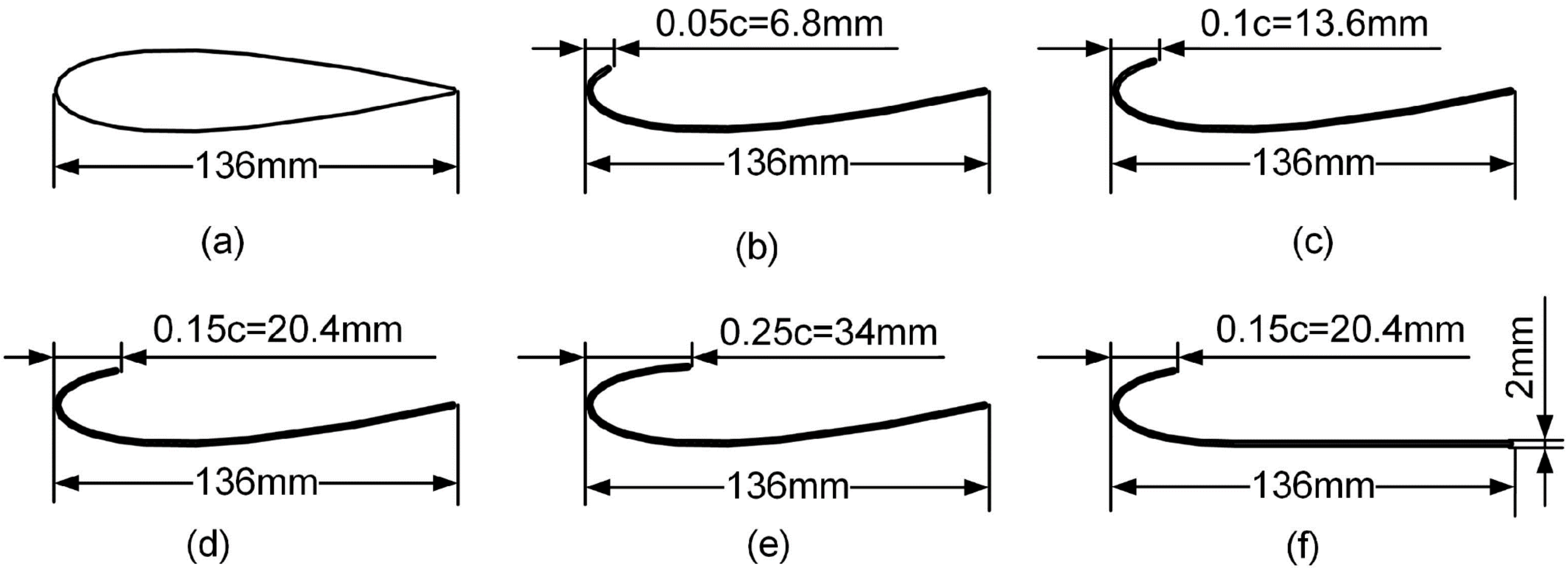

Figure 11. J-blade with different openings

Research Objectives

according to
topics

- This research aims to create an **optimized J-shaped blade** to enhance the Darrieus turbine's performance by encouraging resilient, sustainable infrastructure that is built and run to have the least negative effects on the environment that maintains the Darrieus turbine's performance while improving starting torque, utilizing a NACA0015 airfoil as a model.
- The earlier research on J-shapes [5-7] and the more recent study [10] concentrated **on blades with a hollow and hair-like form**; however, they did not investigate the inner shape of the construction. Thus, this study evaluates the performance of J-shaped blades with an **interior-filled construction.**

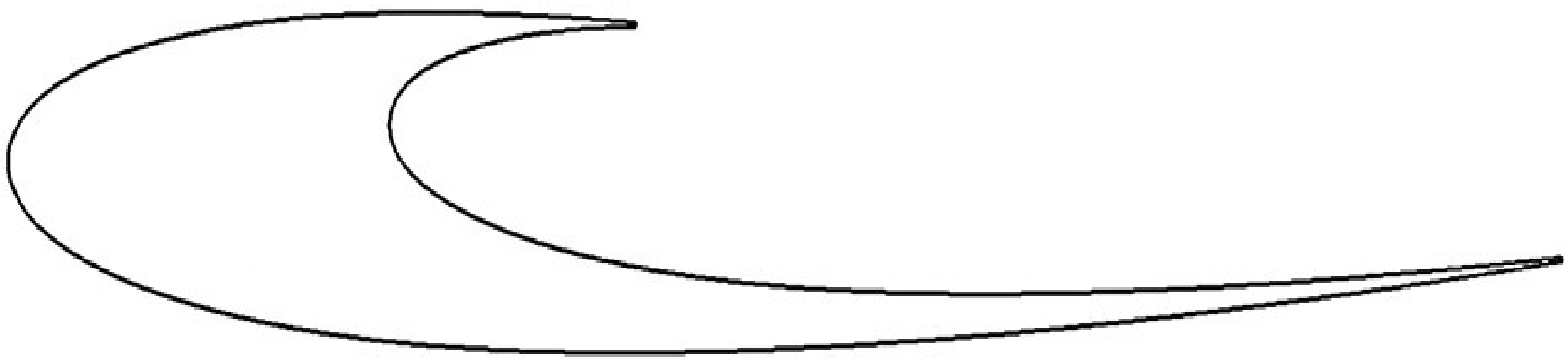

Figure 12. J-blade airfoil design

Problem description and setup

according to
topics

- This study leverages the **Finite Volume Fluent Solver** to meticulously investigate the impact of J-shaped configurations on the aerodynamic performance of airfoils for vertical axis wind turbines, employing the **Unsteady Reynolds Averaged Navier Stokes (URANS)** governing equations. The research endeavors to contribute to the understanding of these configurations by presenting a comprehensive analysis through **a turbulent, incompressible, and two-dimensional flow model.**

according to topics

H-Darrieus wind turbine geometry features

according to
topics

Characteristics	Details
No. of blades	3
Rated power	3.5 kW
Chord length	0.4 m
Turbine radius	1.25 m
Blade profile	NACA0015
Solidity	0.48
Wind speed	10 m/s
Reynolds no.	416,254

Table 2. Main geometrical rotor characteristics

Wind turbine governing equations

according to topics

- The validity of the model in this study has been examined by a comparison of the coefficient of power (Cp) vs. tip speed ratio (λ) curve with findings reported in previous studies.

- $C_p = C_m\,(\omega L)/u$ (1)

  $C_p = C_m\,(\omega R)/u$ (2)

  $\lambda = (\omega R)/u$ (3)

  $C_p = C_m\,\lambda$ (4)

according to
topics

Gromeka acceleration vector (m/s^2) is the rate of change of angular momentum [16]. According to [17], The total external torque acting on a system of particles equals the rate of change of the system's total angular momentum.

The torque created on the turbine is evaluated by measuring the Gromeka acceleration vector.

For a 2D flow, the velocity (u) may be defined as

$$\vec{u} = \begin{pmatrix} u \\ v \\ 0 \end{pmatrix} \qquad (5)$$

And we can determine vorticity using equation (6).

$$\vec{\xi} = \nabla \times \vec{u} = \begin{pmatrix} \xi_x \\ \xi_y \\ \xi_z \end{pmatrix} \qquad (6)$$

For a 2D flow,

$$\vec{\xi} = \nabla \times \vec{u} = \begin{pmatrix} 0 \\ 0 \\ \frac{\partial v}{\partial x} - \frac{\partial u}{\partial y} \end{pmatrix} \quad (7)$$

To extract the Gromeka acceleration vector $\vec{G} = \vec{\xi} \times \vec{u}$
(8)

For a 2D flow, the Gromeka acceleration vector may be defined as

$$\vec{G} = \begin{pmatrix} v\xi_Z \\ -u\xi_z \\ 0 \end{pmatrix} = \begin{pmatrix} v(\frac{\partial v}{\partial x} - \frac{\partial u}{\partial y}) \\ -uv(\frac{\partial v}{\partial x} - \frac{\partial u}{\partial y}) \\ 0 \end{pmatrix} \quad (9)$$

according to
topics

To determine the Gromeka acceleration vector magnitude, this equation is utilized.

$$\overrightarrow{|G|} = \sqrt{\left(v\left(\frac{\partial v}{\partial x} - \frac{\partial u}{\partial y}\right)\right)^2 + \left(-u\left(\frac{\partial v}{\partial x} - \frac{\partial u}{\partial y}\right)\right)^2} \quad (10)$$

$$= \sqrt{\left(\left(\frac{\partial v}{\partial x} - \frac{\partial u}{\partial y}\right)\right)^2 \times (u^2 + v^2)} \quad (11)$$

$$= \sqrt{(|\vec{\xi}|)^2 \times (|\vec{u}|)^2} \quad (12)$$

Numerical details and solver setup

according to
topics

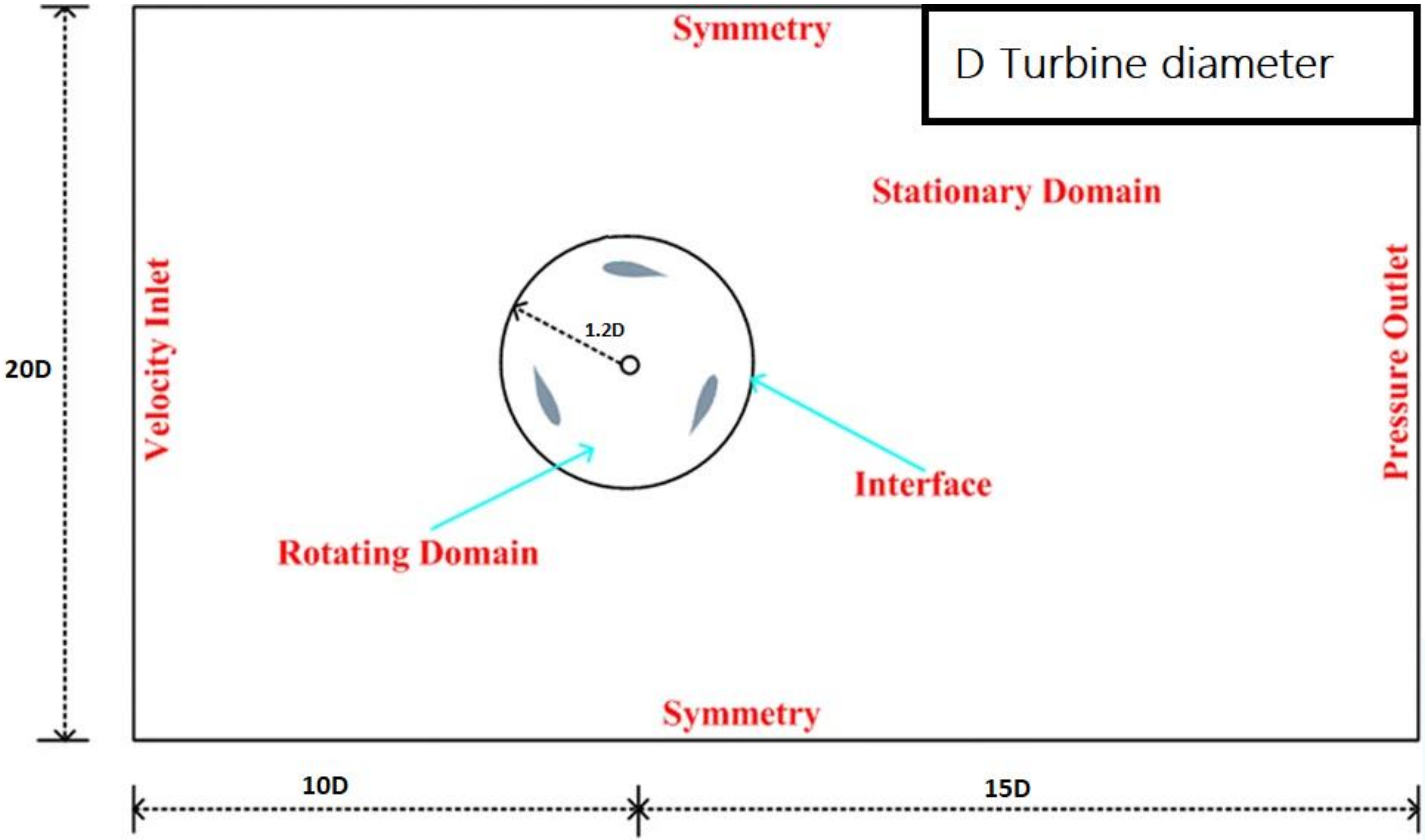

Figure 13. Computational domain

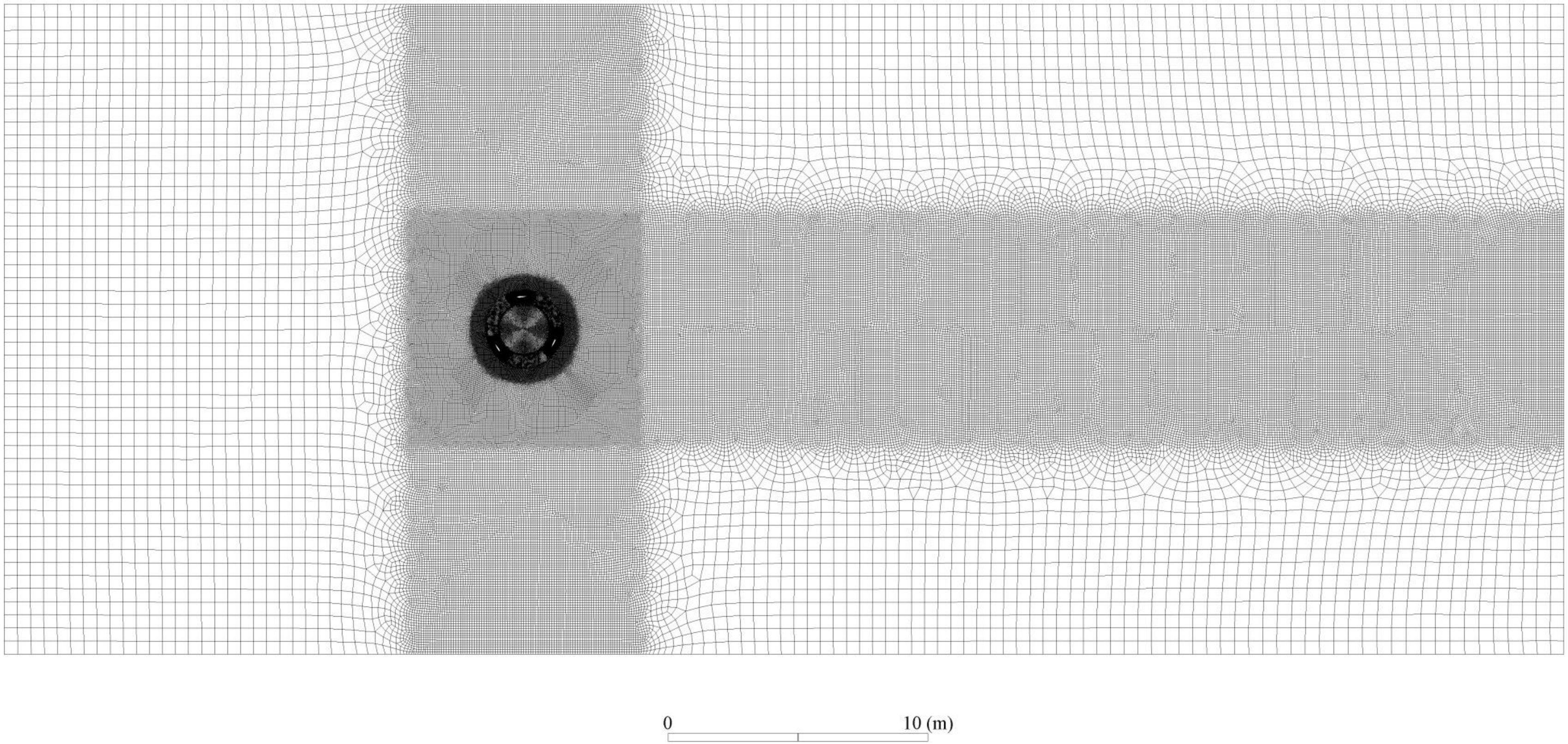

Figure 14. Grid distribution around NACA 0015

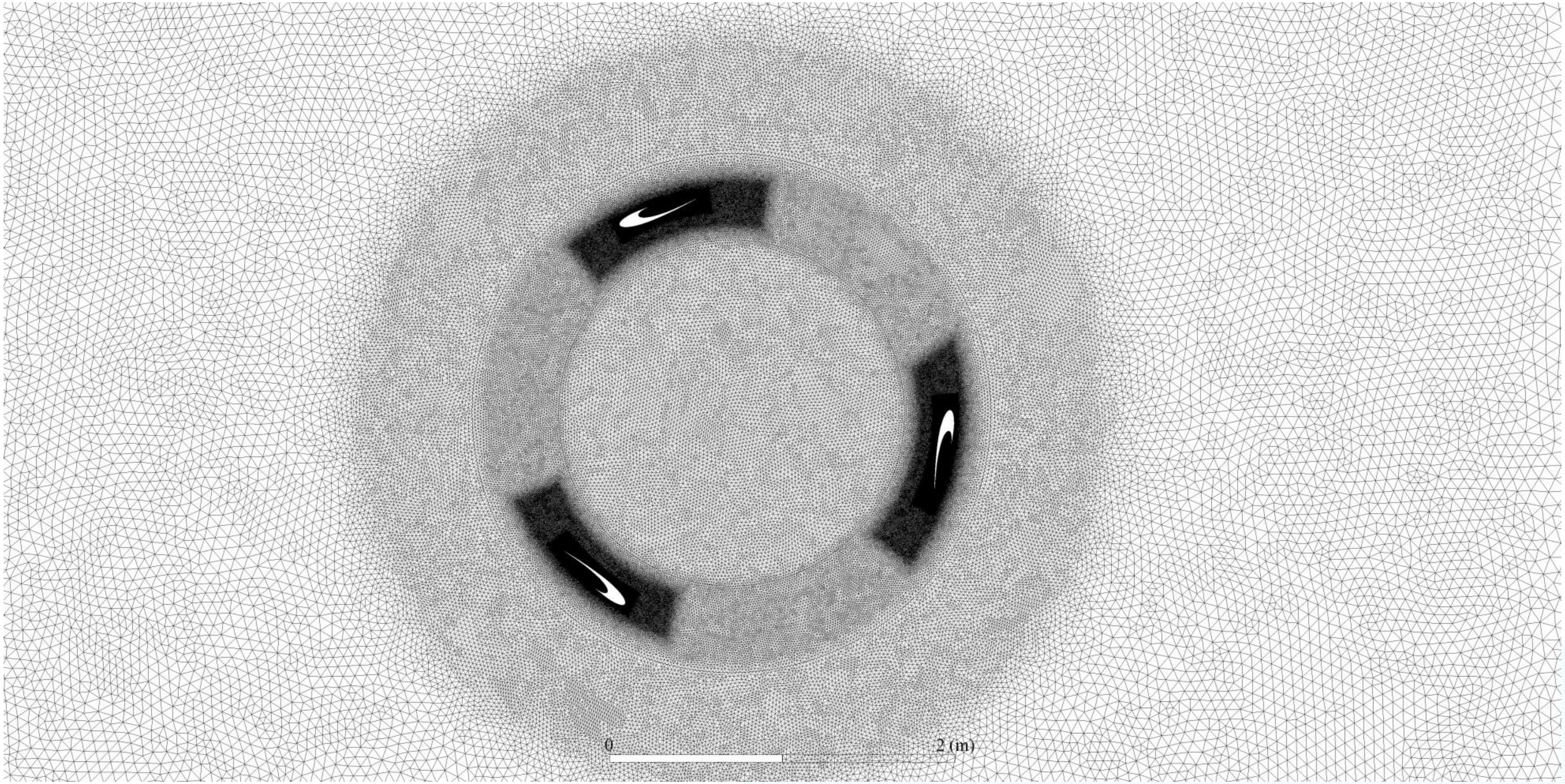

Figure 15. Grid distribution around NACA 0015

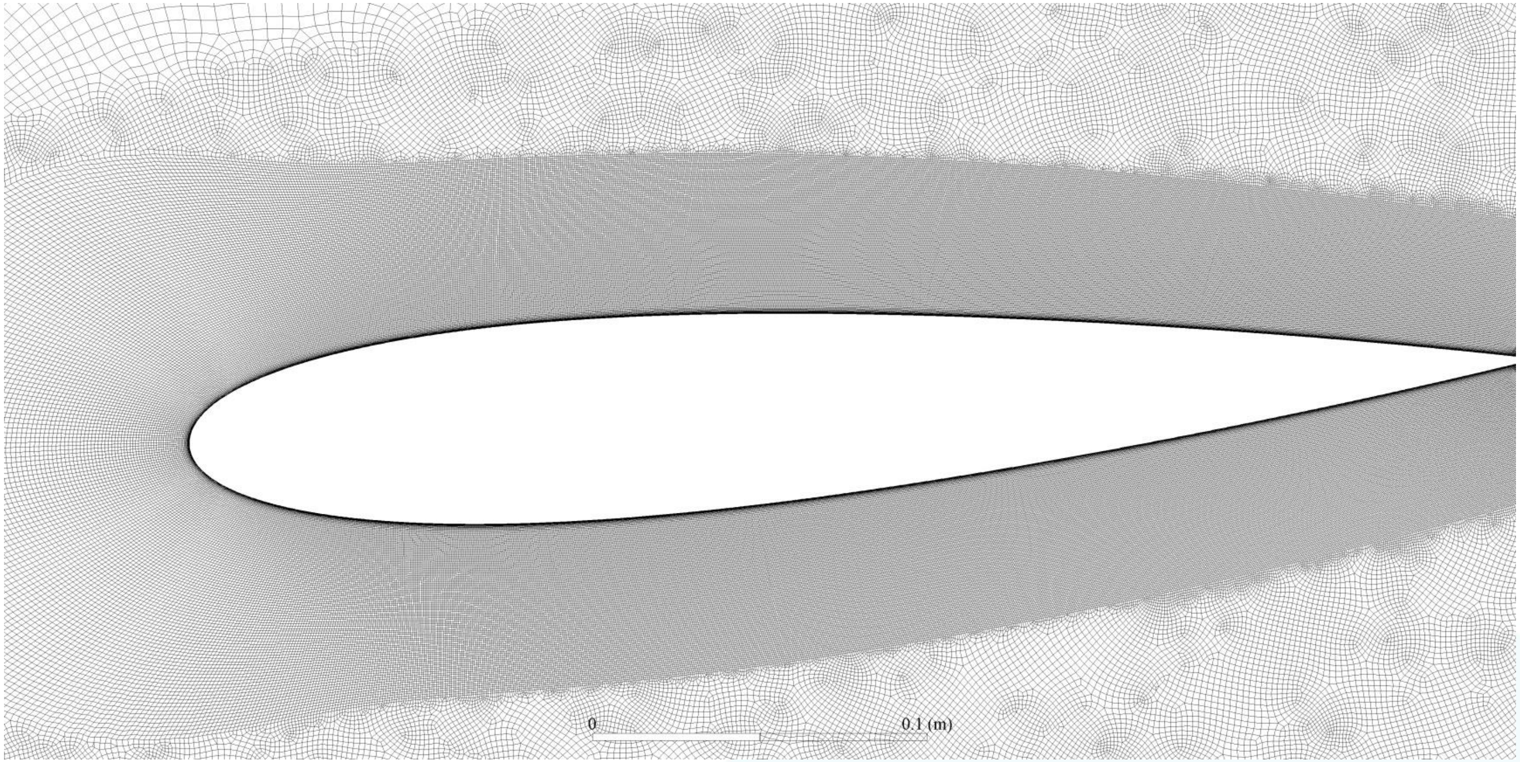

Figure 16. Grid distribution around NACA 0015

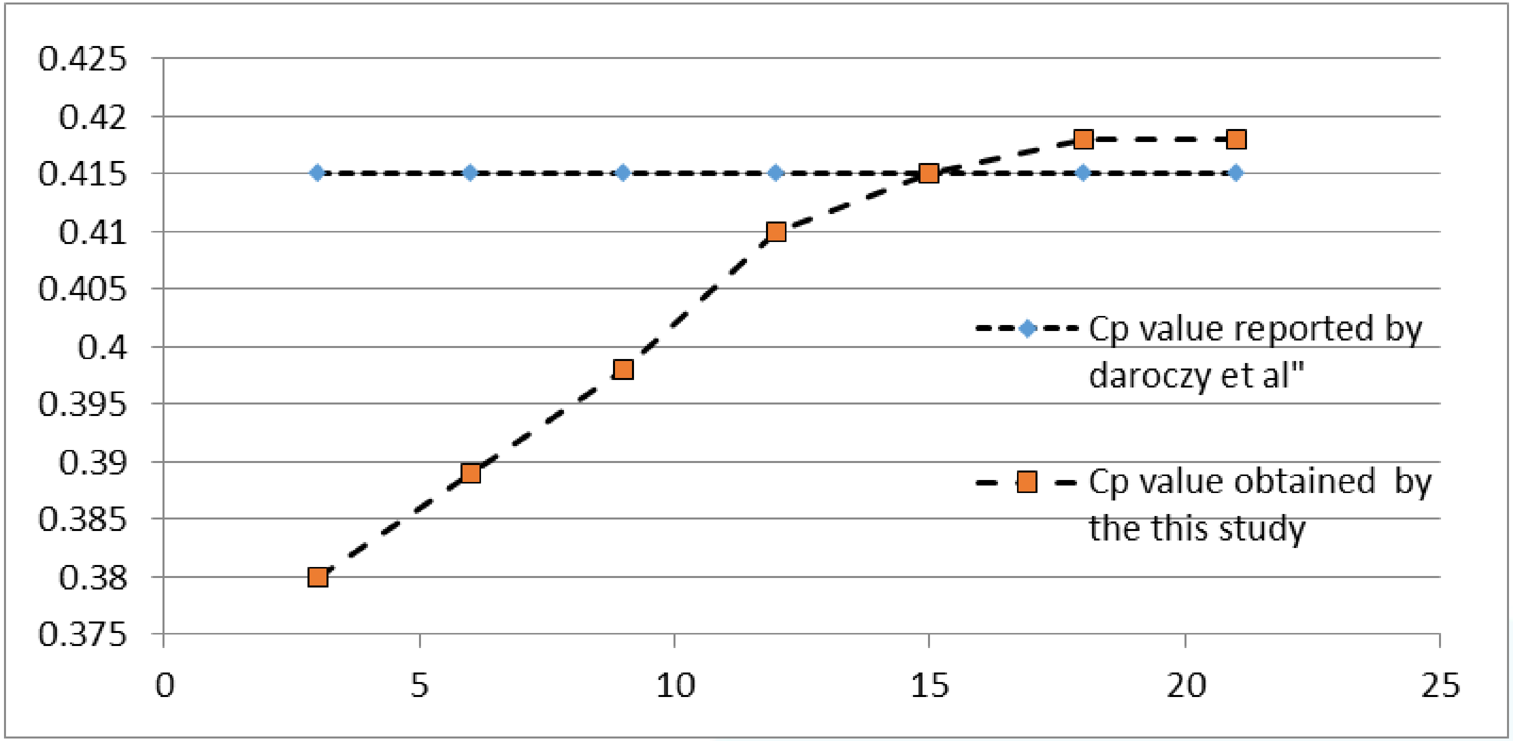

Figure 17. Mesh independence study

Numerical setup

according to
topics

Simulation assumptions:

- k-ω SST model.
- SIMPLE algorithm .
- Utilizing a second-order upwind approach.
- The outlet boundary is represented as a pressure outlet.
- the surface of the airfoil is described as a non slip wall.
- the inlet boundary is represented as a velocity inlet.

according to
topics

Azimuthal increments served as the foundation for the transient simulation's time step. To replicate the five λ of interest, five unique rotating speeds w (rad/s) were considered: 0.2 (to examine the starting torque), 1.25, 1.6, 2 and 2.5.
, the time step in the present investigation was defined as

$$\Delta t = 2\pi\,\Delta\theta/(360\omega) \qquad (13)$$

Where Δt time is step size and Δθ is azimuthal increment. $(0.5\,^{0})$ was utilized as the azimuthal increment at each time step in agreement with comparable numerical work published in [11]. Equation (13) was used to compute the appropriate time steps depending on the values of ω and Δθ.

λ	$\omega(rad/s)$	Time step (s)
0.2	1.6	0.005454
1.25	10	0.0008727
1.6	12.8	0.0006817
2	16	0.0005454
2.5	20	0.0004363

Table 3. ω and Δt for different λ.

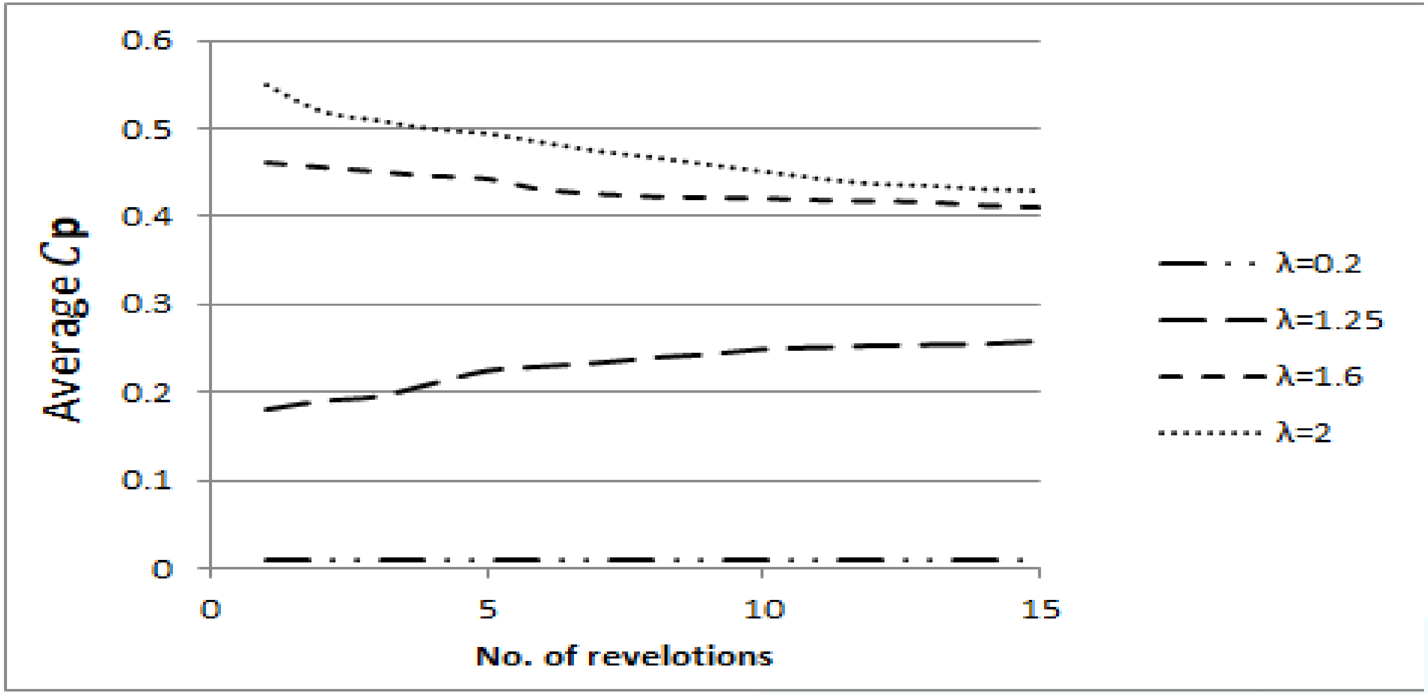

Figure 18. Number of revolutions until convergence of simulated Cp values at various λ.

VERIFICATION AND VALIDATION

according to topics

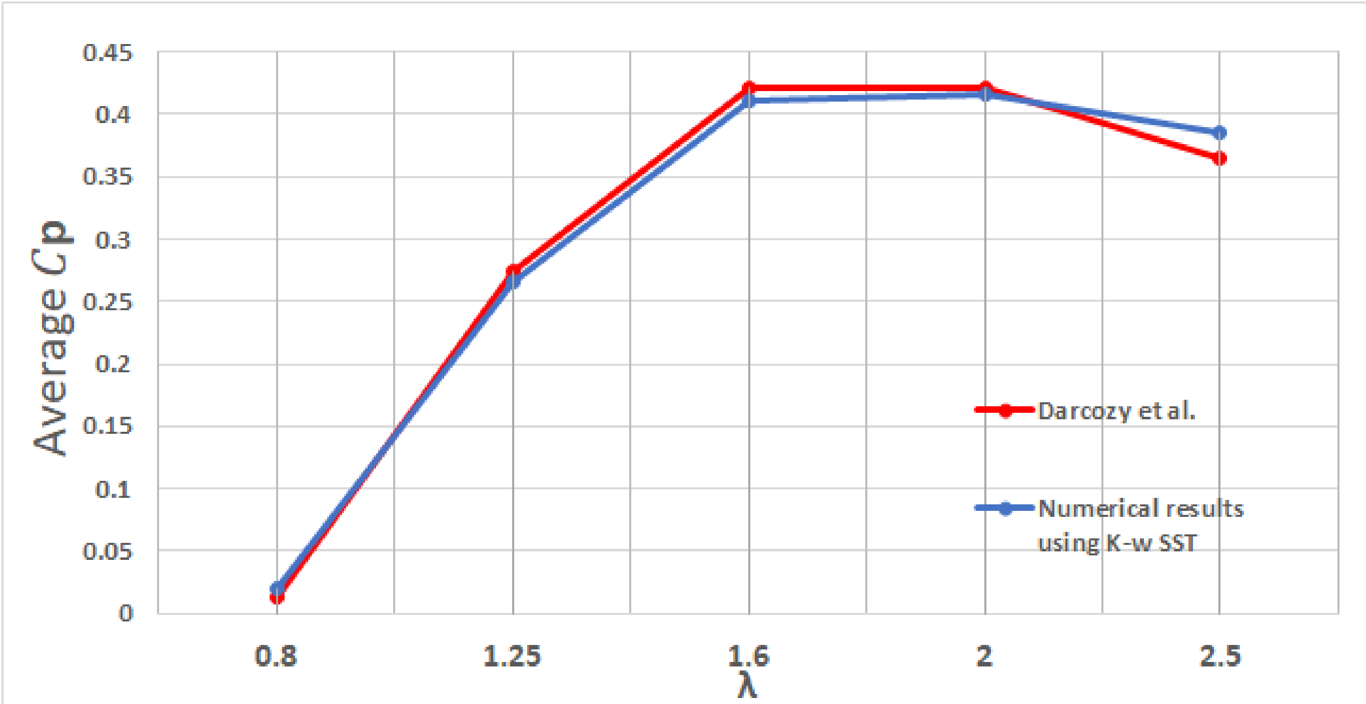

Figure 19. C_P comparison between the present study and Daróczy et al. at different λ

J-BLADE CONFGURATION

according to
topics

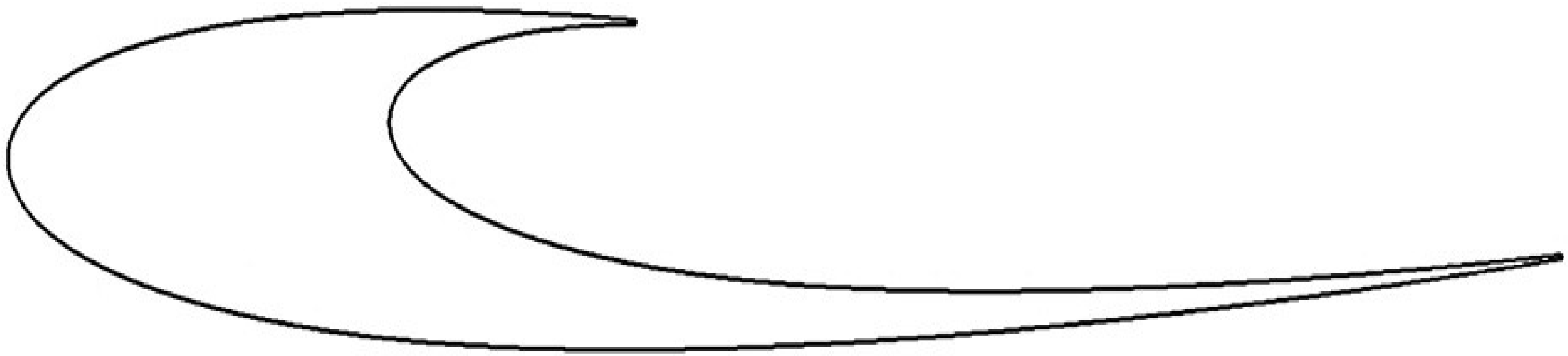

Figure 20.(a) J-blade airfoil design

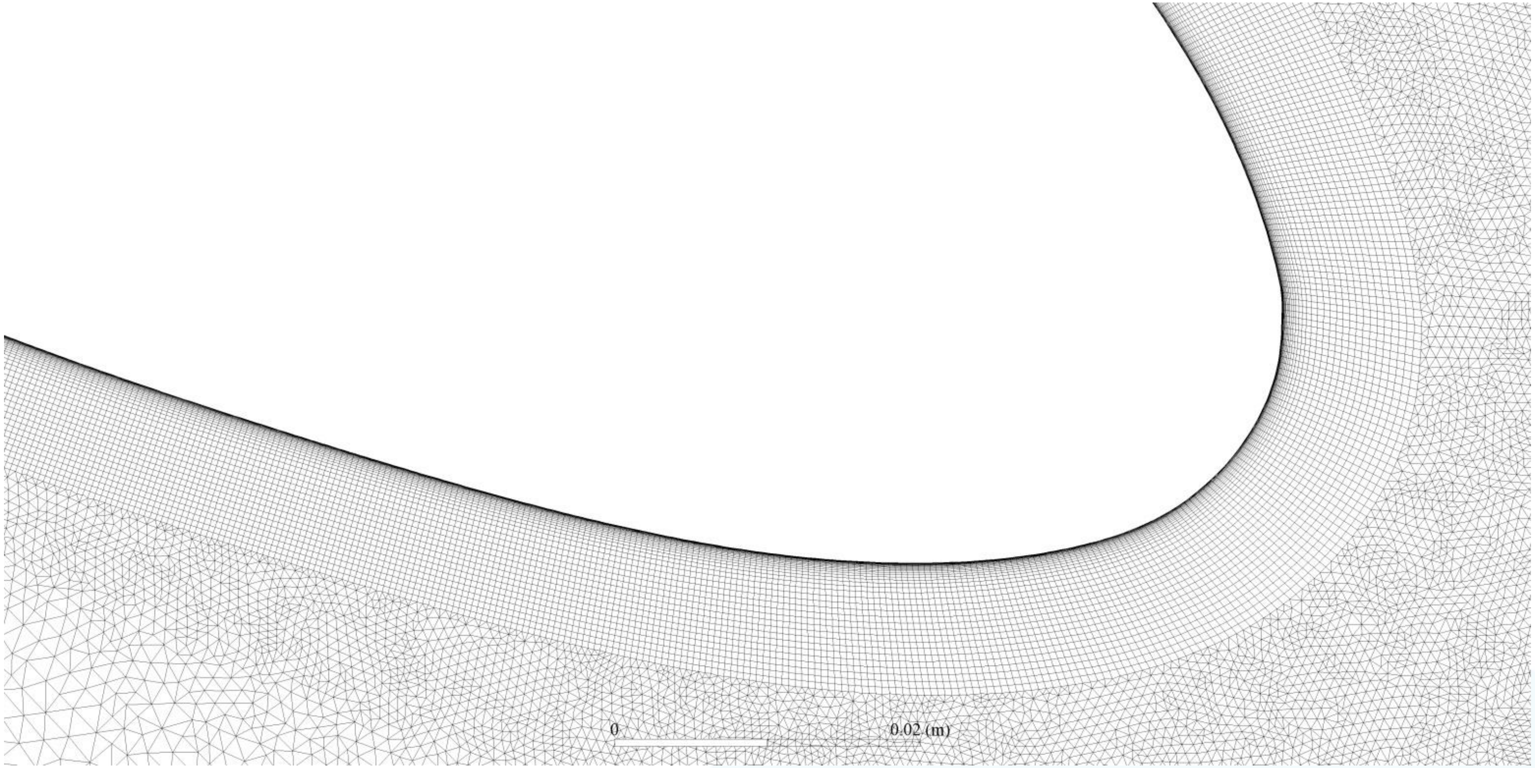

Figure 20. (b) the grid distribution

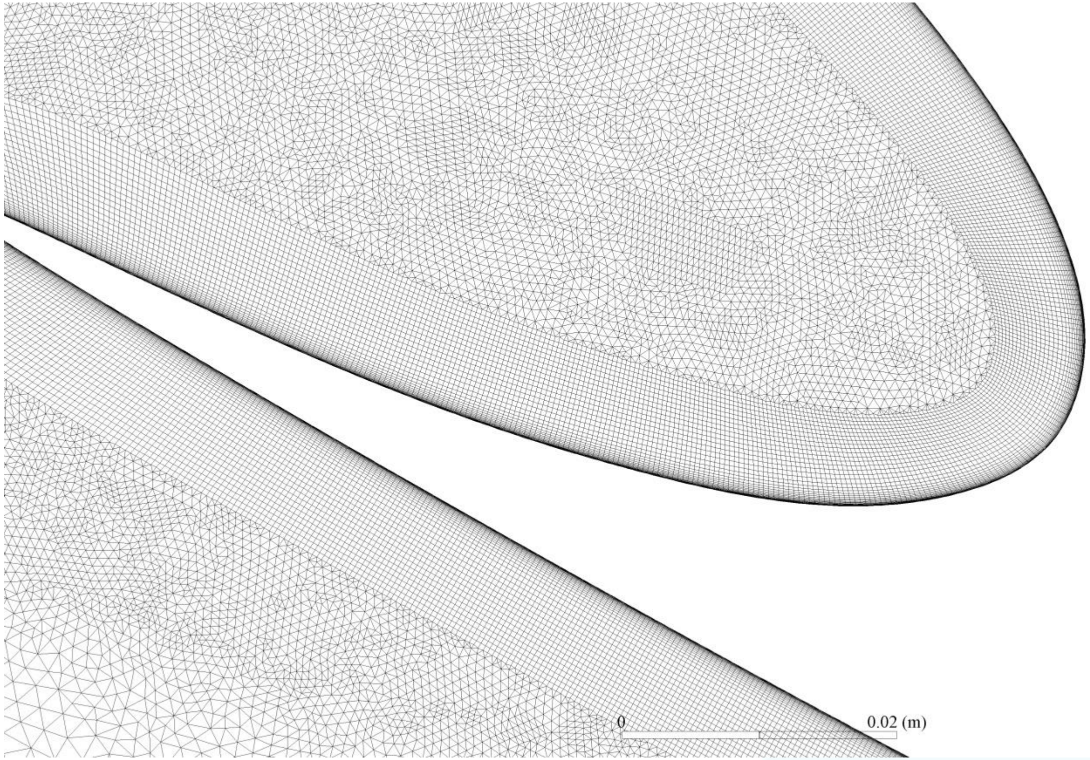

Figure 20. (b) the grid distribution

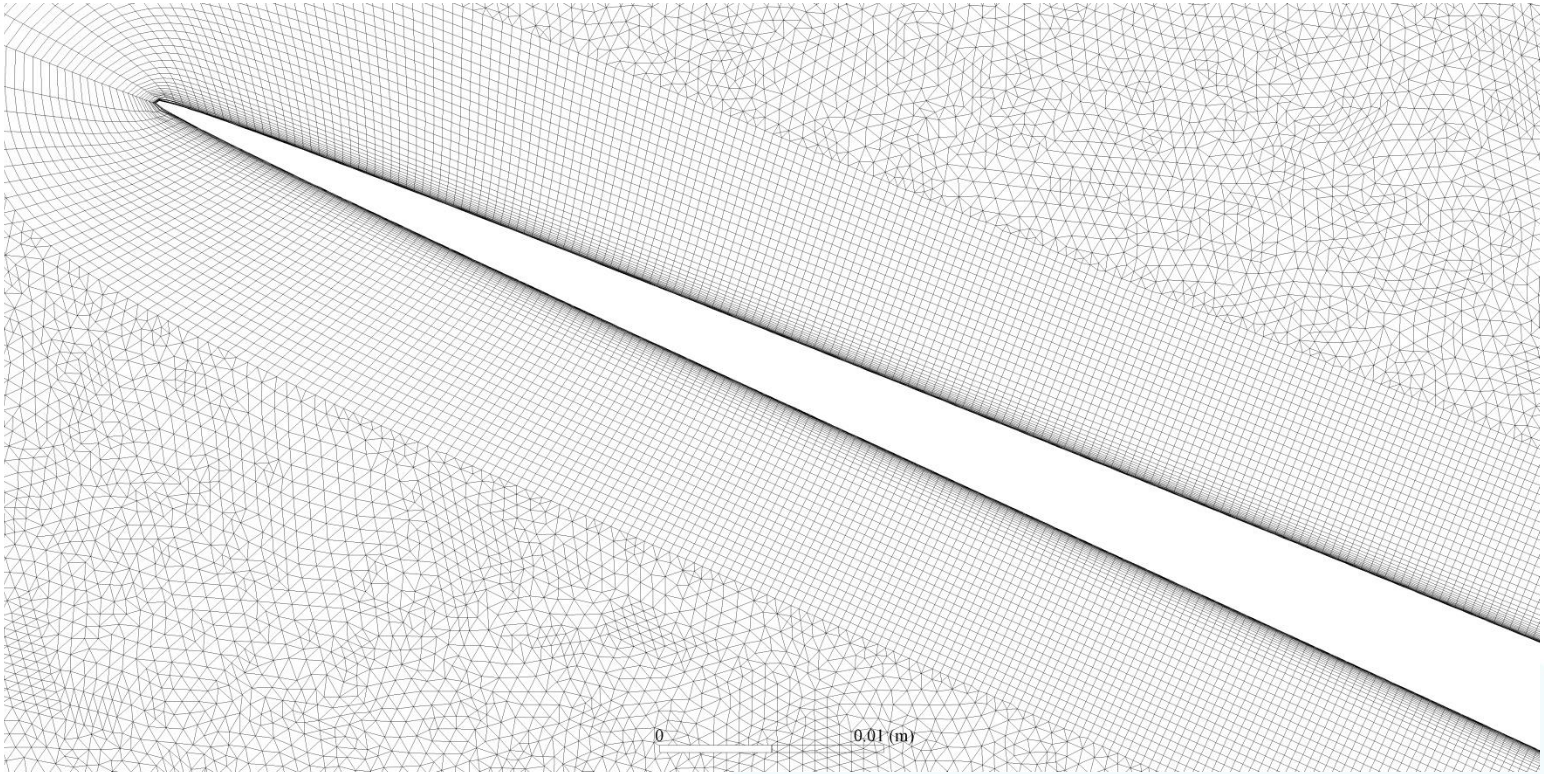

Figure 20. (b) the grid distribution

RESULTS AND DISCUSSION

according to
topics

Standard operating conditions

according to
topics

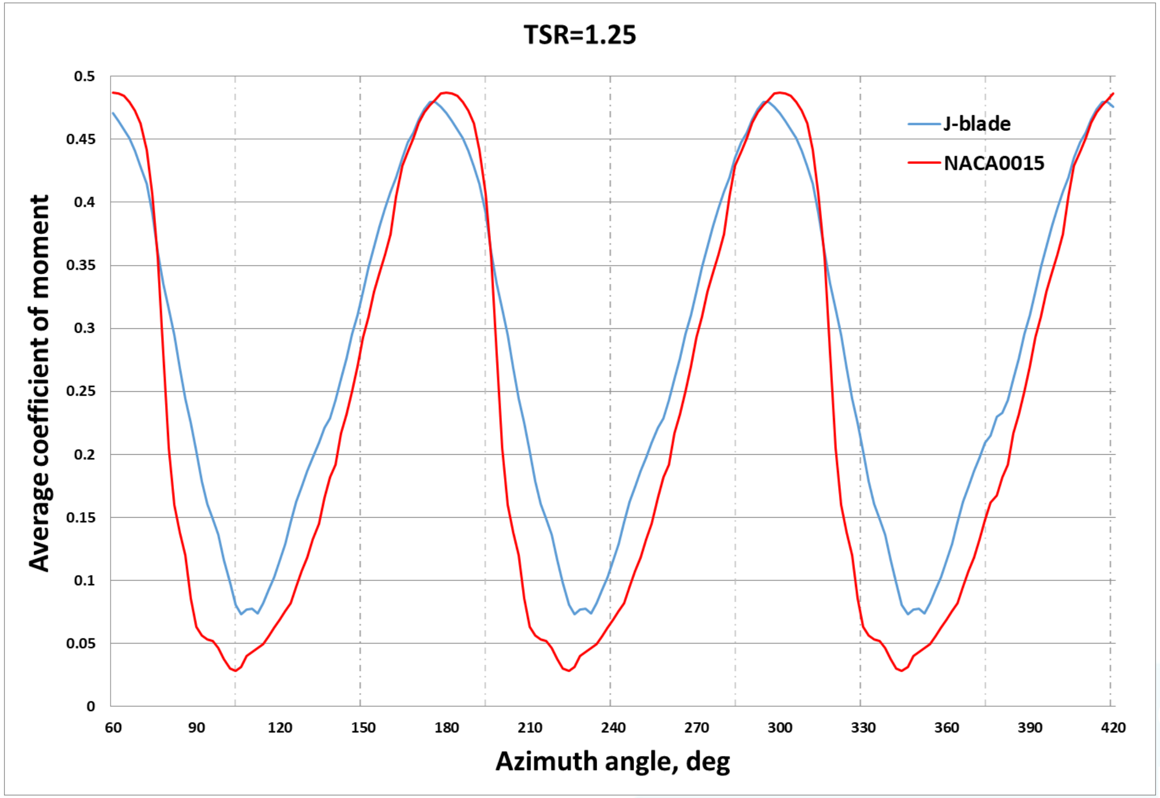

Figure 23. Cm comparison between NACA0015 (red) and J-blade (blue) at λ =1.25(a)

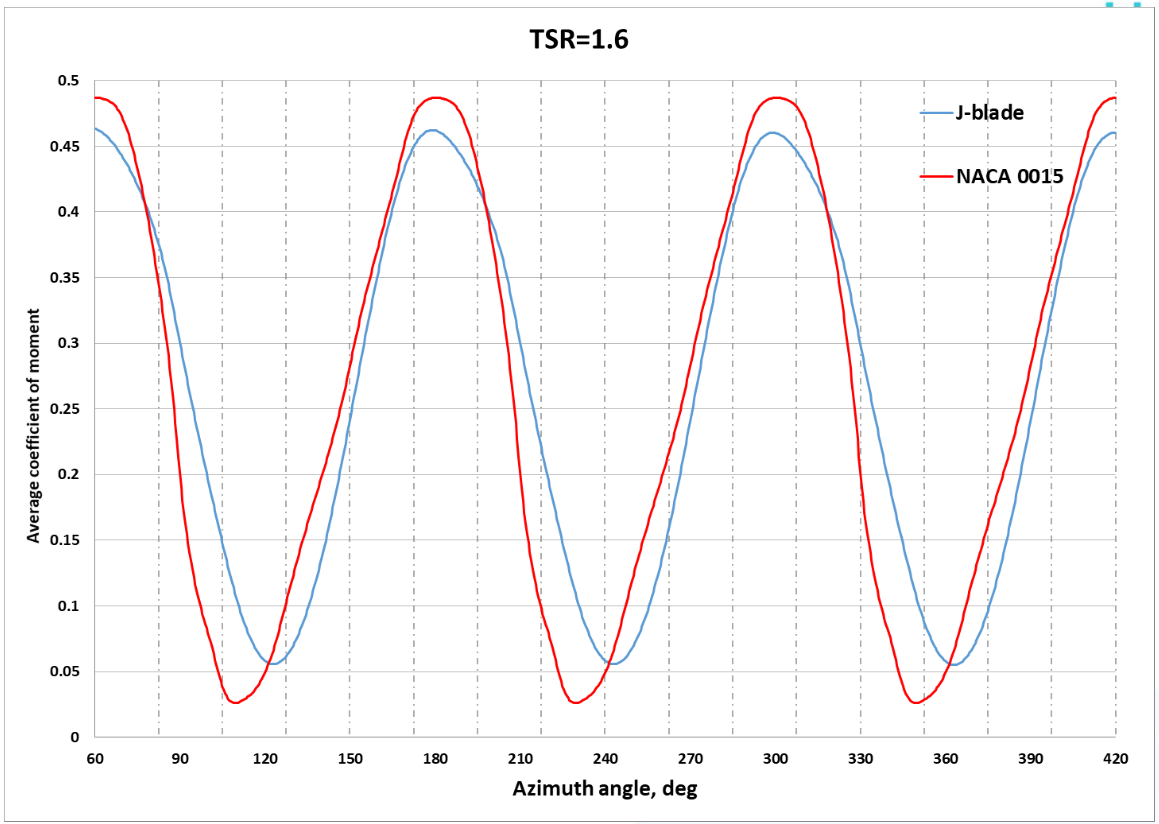

Figure 24. Cm comparison between NACA0015 (red) and J-blade (blue) at $\lambda = 1.6$ (b)

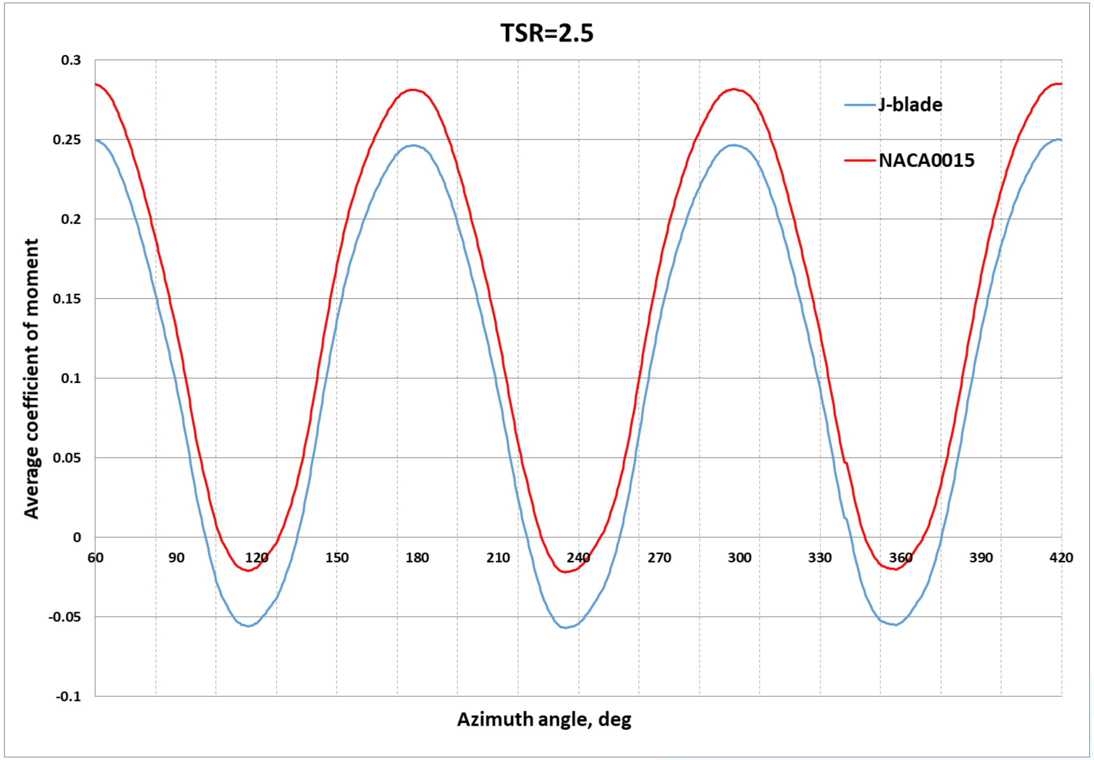

Figure 25. Cm comparison between NACA0015 (red) and J-blade (blue) at λ =2.5(c)

- The torque values of the J-blade airfoil and the NACA0015 airfoil are comparable. For the majority of the operating zone, the J-blade airfoil outperformed the NACA0015 airfoil in terms of performance.

- The J-blade airfoil generated torque equivalent to the NACA0015 airfoil at λ of 1.25 and 1.6, but it was more uniform, which added benefits in terms of energy generation and mechanical stresses. Nevertheless, the J-blade airfoil's performance began to lag behind that of the NACA0015 airfoil at λ of 2.5.

according to topics

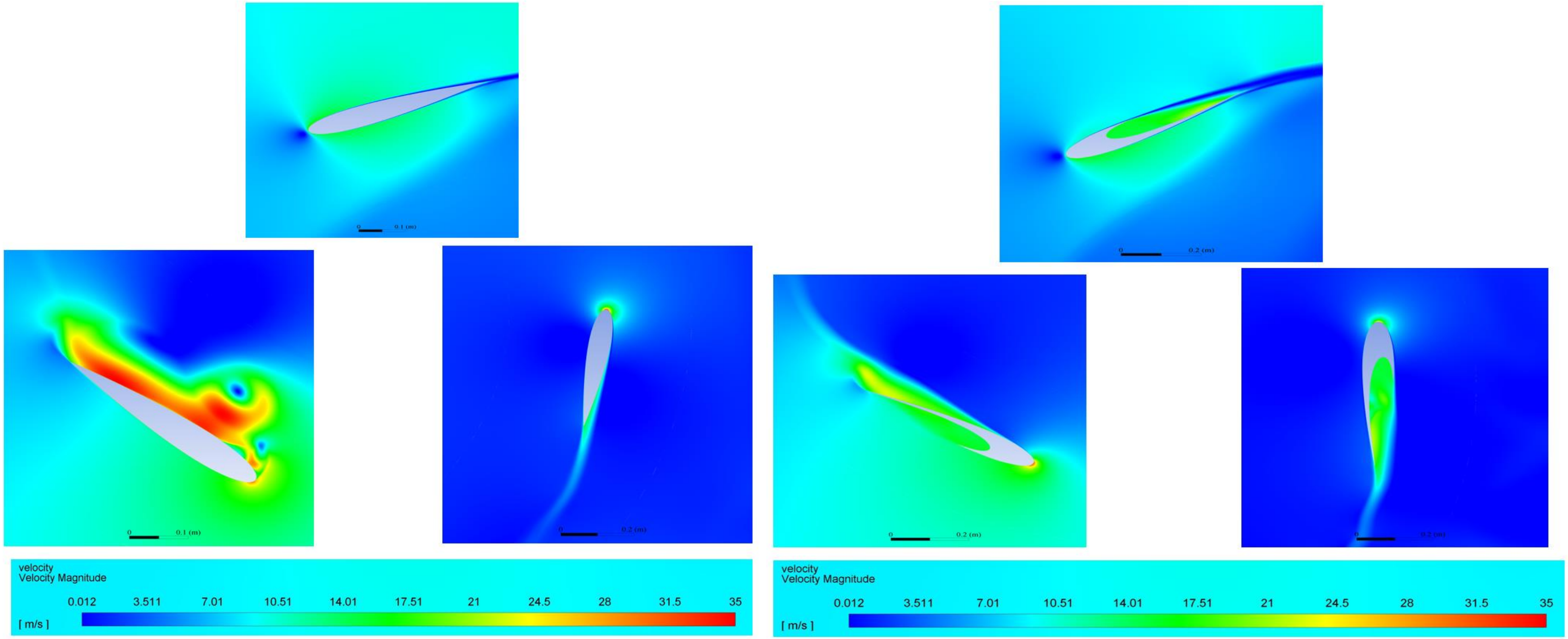

Figure 26. Contours of the velocity magnitude at λ =1.6 around the airfoil for NACA0015 (left) and J-blade (right)

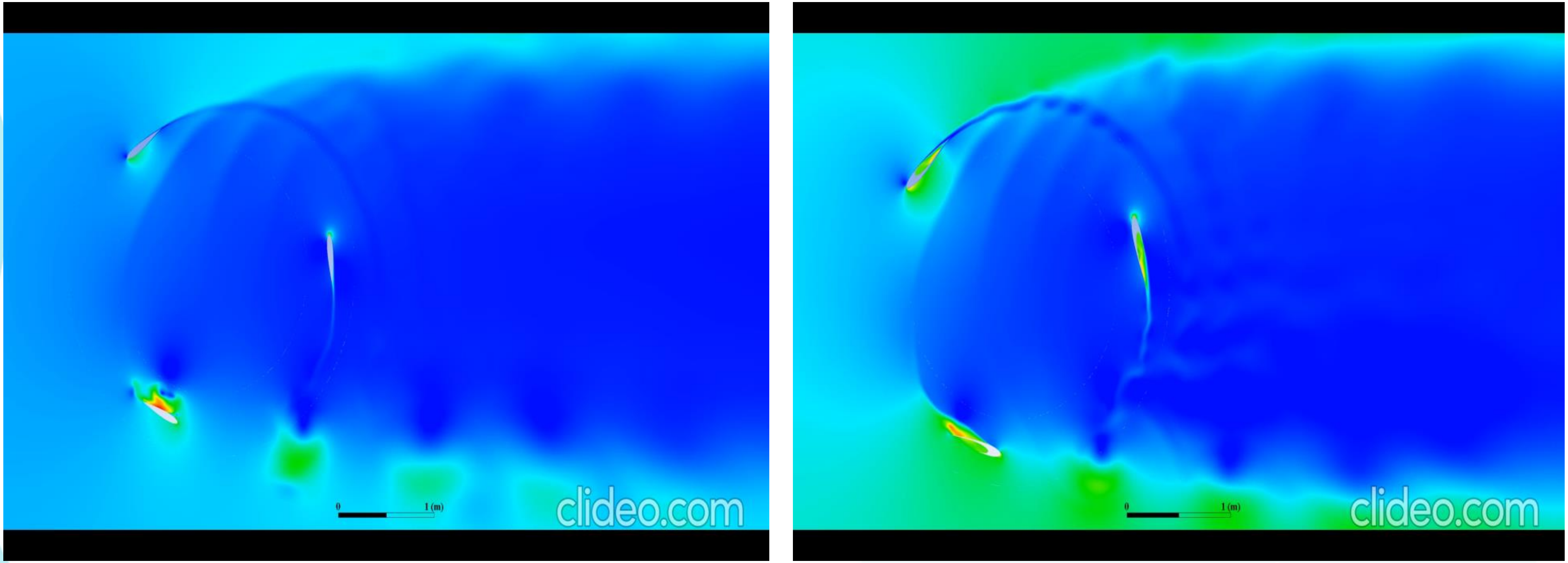

Figure 26. Contours of the velocity magnitude at λ =1.6 around the airfoil for NACA0015 (left) and J-blade (right)

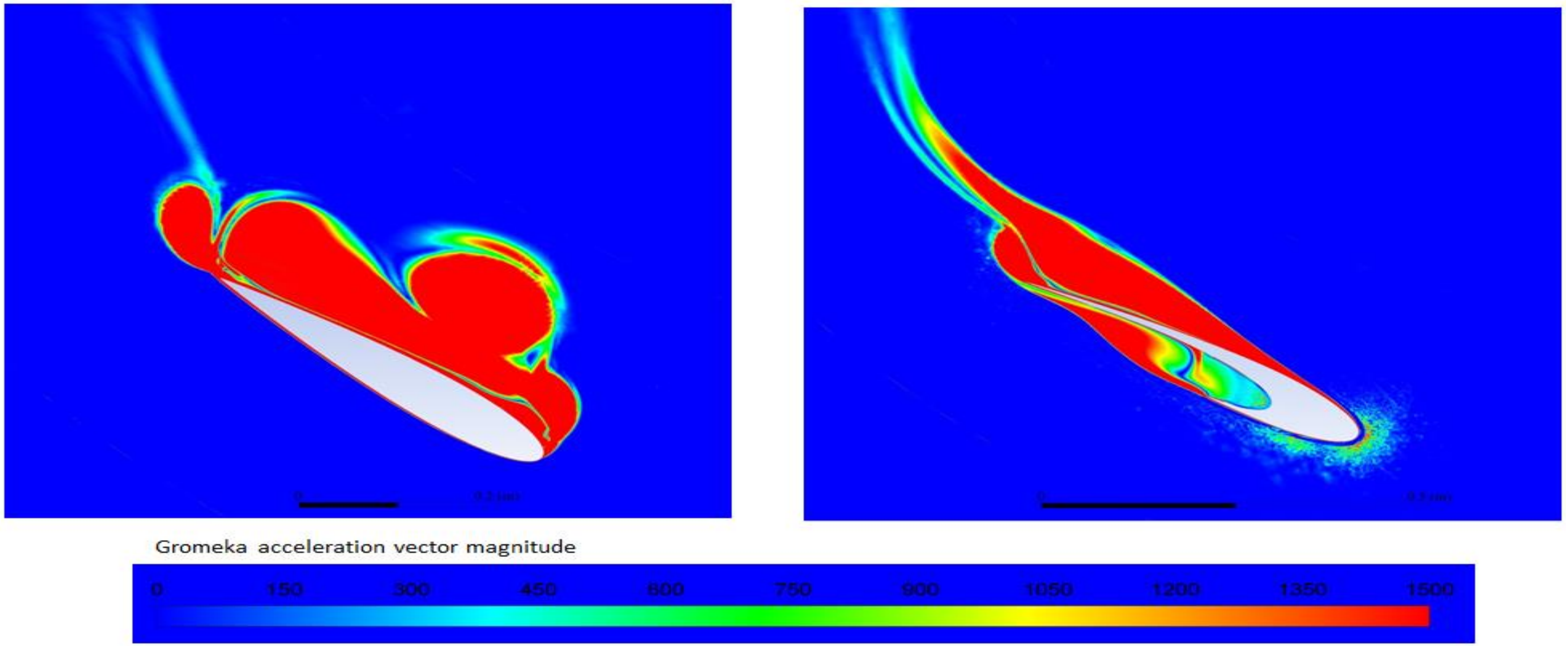

Figure 27. Contours of Gromeka acceleration vector magnitude in leeward region At λ =1.6 Around blade for NACA0015(left) and J-blade (right)

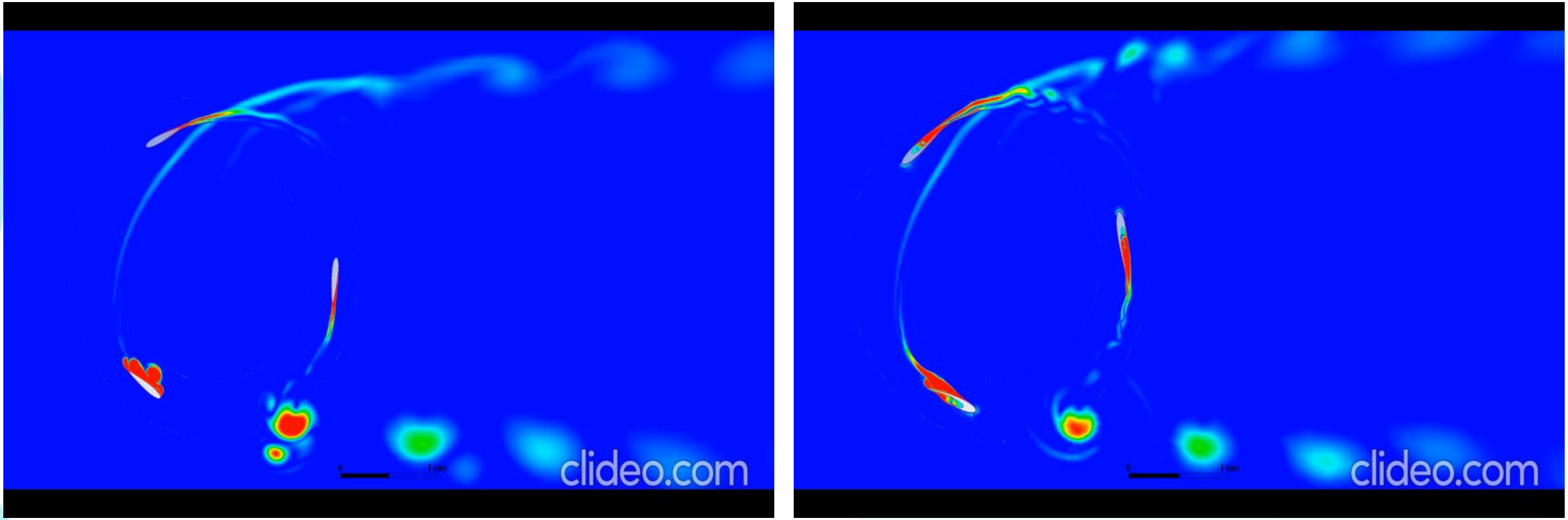

Figure 27. Contours of Gromeka acceleration vector magnitude in leeward region At λ =1.6 Around blade for NACA0015(left) and J-blade (right)

- On the pressure side, the J-blade airfoil displays vortexes, yet the flow characteristics are not significantly affected by this cut. Figure 24 illustrates how the slight increase in drag causes just a slight reduction in torque in that area.

- With regard to the contours in the leeward zone, both airfoils exhibit significant flow separation. It is noteworthy, however, that the J-blade design exhibits the lowest vortex production, as shown in Figures 26, 27.

according to topics

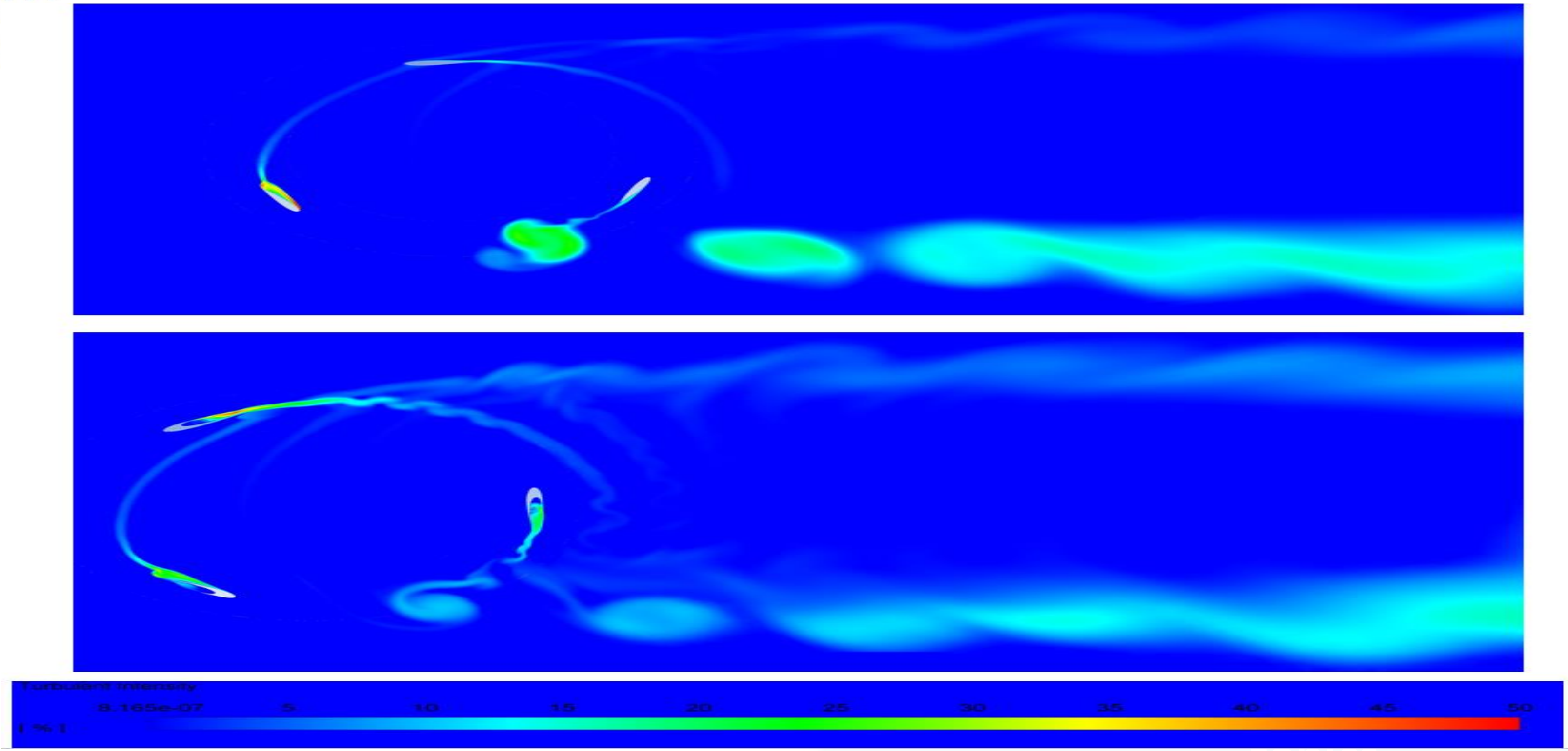

Figure 28. Contours of turbulence intensity λ =1.6 around the turbine for NACA0015 (upper) and J-blade (down)

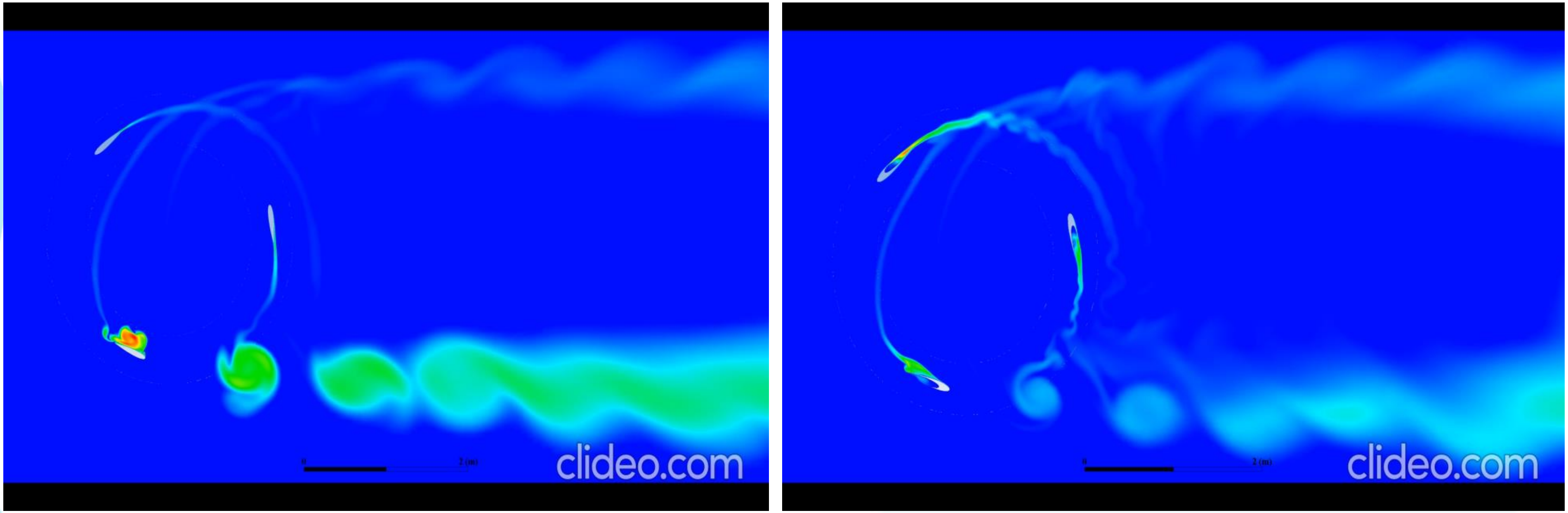

Figure 28. Contours of turbulence intensity λ =1.6 around the turbine for NACA0015 (upper) and J-blade (down)

- Thus, with λ = 1.6, Figure 28 displays examples of the turbulence fields for this airfoil. The vortex shedding in the leeward zone is a substantial influence detected in the velocity field.

- The Gromeka acceleration vector contour charts given in Figure 27 indicate how the J-blade airfoil greatly lowers the creation of vortices and shedding during passage in the leeward zone.

- In Figure 28, the contour plots of turbulence intensity are provided to offer a more complete study of the effect of this vortex production.

- Thus, combining both factors results in a uniform wake behind the turbine for the J-blade airfoil.

- Because turbulence from one turbine impacts the energy production of the next, we may use this consistency by deploying more and more wind turbines in the same geographical location, resulting in higher energy yields and cost savings.

- The instability in the wake raises the mechanical stresses and lowers the turbine's energy production.

according to topics

Starting Torque

according to
topics

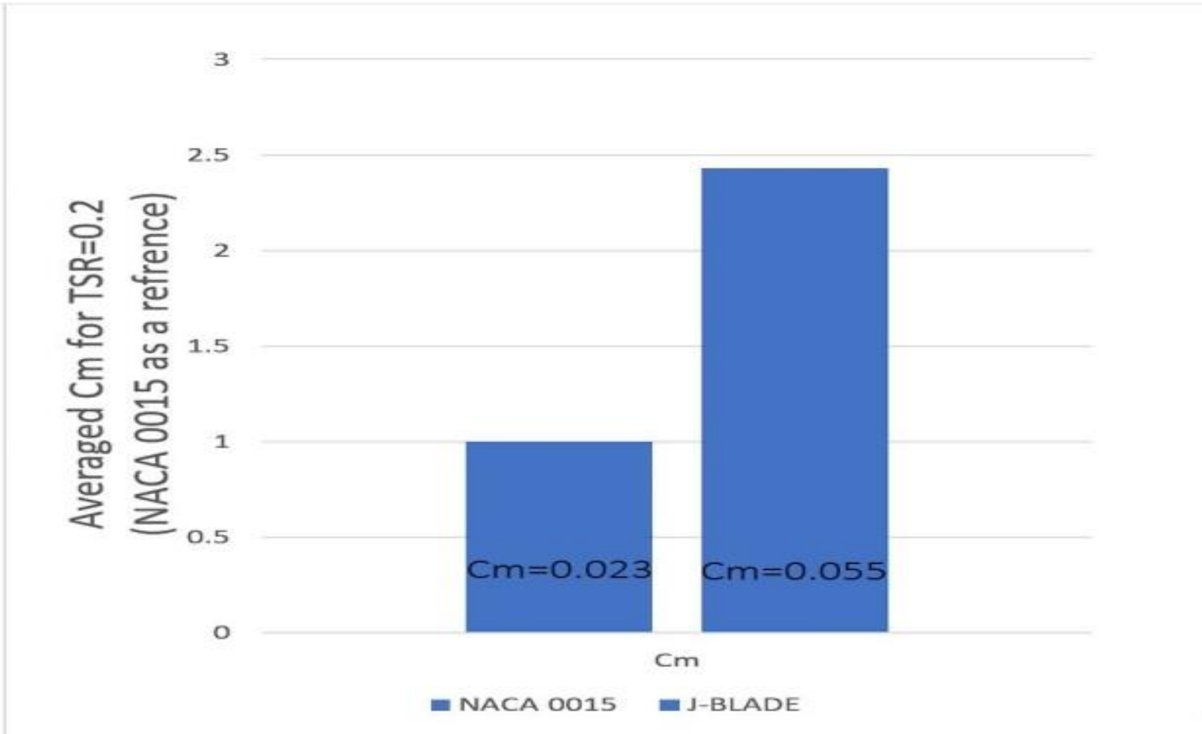

Figure 20. Averaged Cm for λ=0.2 of NACA0015 (left) and J-blade (Right)

- The simulated airfoil reveals that the J-blade airfoil has a **142%** increase in starting torque compared to the NACA0015 airfoil, as shown in figure 20. This rise in initial torque originates from the airfoil’s cut, which causes additional drag going through the leeward zone.

- The J-blade consequently acts as a consequence of simultaneous lift and drag forces. In addition, the J-blade's notch provides drag force that helps the blades rotate more swiftly. Conversely, it enhances rotational efficiency by creating greater torque by harnessing the same wind more often.

according to topics

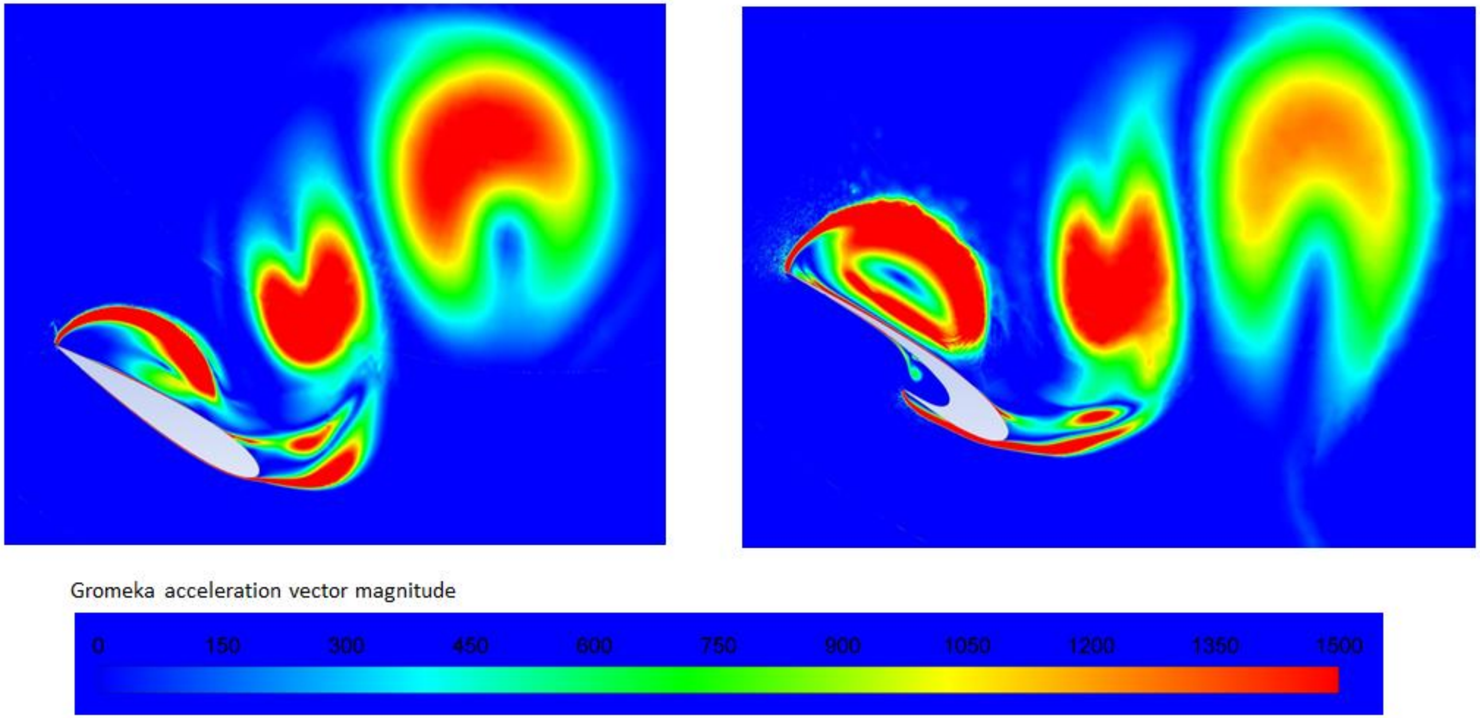

Figure 21. Contours of the Gromeka acceleration vector in leeward region at λ =0 .2 around the airfoil for NACA0015 (left) and J-blade (right)

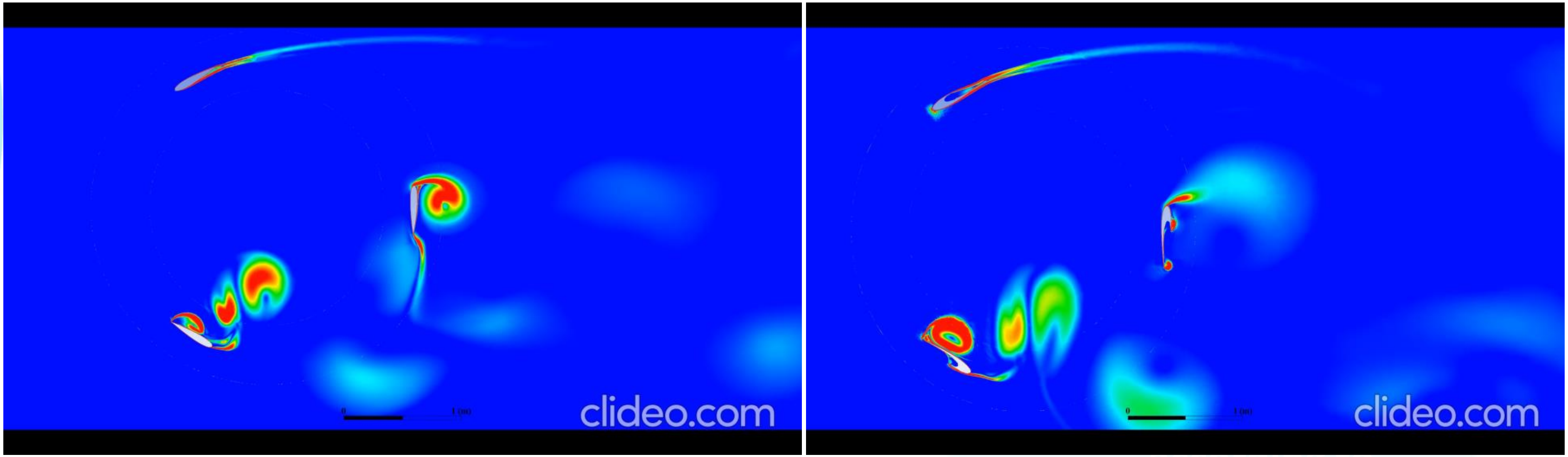

Figure 21. Contours of the Gromeka acceleration vector in leeward region at λ =0 .2 around the airfoil for NACA0015 (left) and J-blade (right)

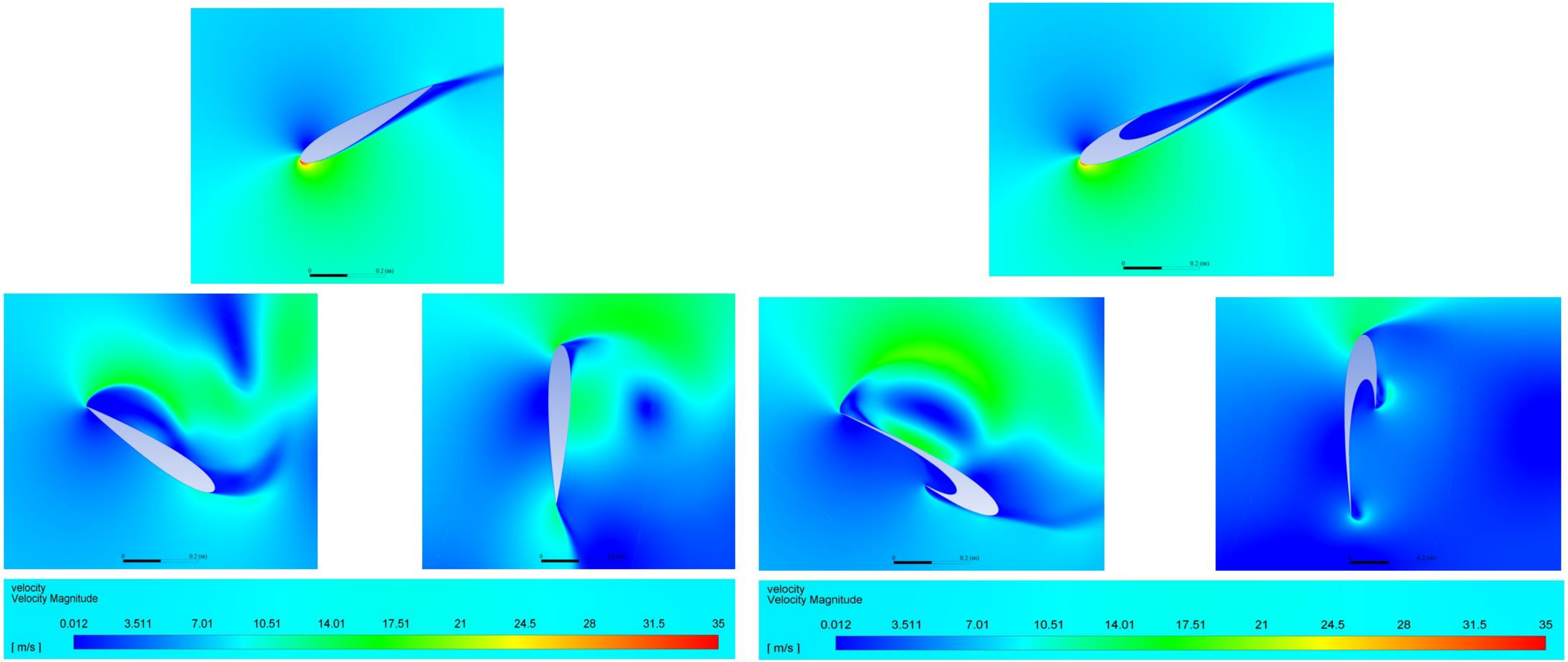

Figure 22. Contours of the velocity magnitude at λ =0 .2 around the airfoil for NACA0015 (left) and J-blade (right)

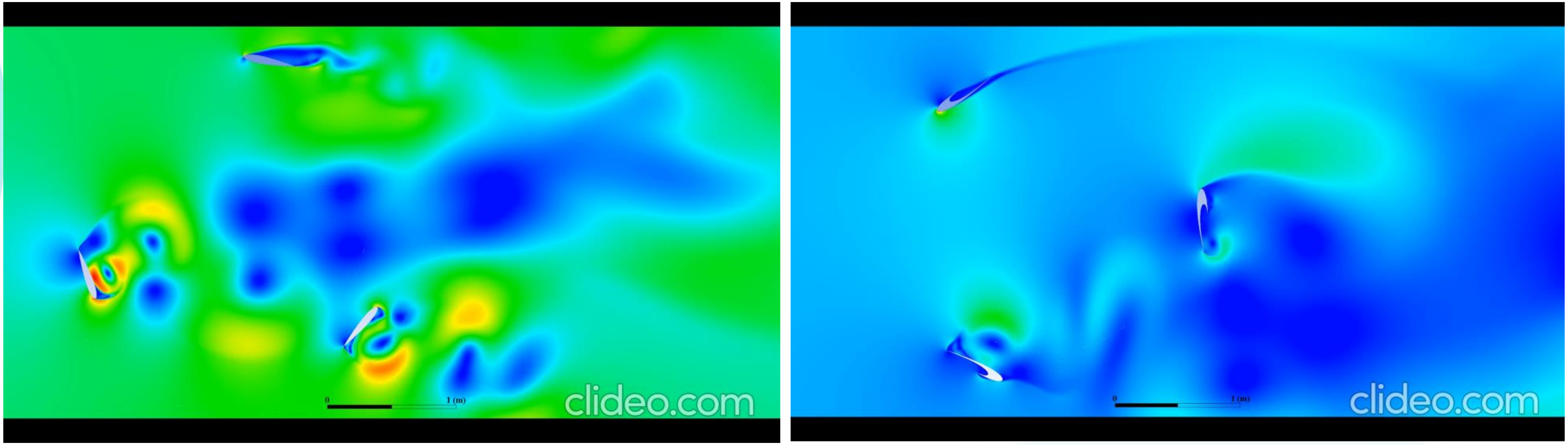

Figure 22. Contours of the velocity magnitude at λ =0 .2 around the airfoil for NACA0015 (left) and J-blade (right)

Conclusions:

This research introduces and investigates the performance of an enhanced J-shaped blade for the Darrieus turbine, specifically tailored to urban environments. Using the URANS governing equations, a turbulent, incompressible, two-dimensional flow model was developed, focusing on both experimental validation and numerical models. The study systematically compared the proposed J-shaped blade with traditional NACA0015 blades, reproducing the Darrieus turbine to validate the numerical model in the range of low λ (λ = 1.5). The findings reveal that:

1.The J-shaped blade not only preserves power generation at the maximum efficiency point but also enhances uniformity, offering advantages in terms of fatigue stresses. This characteristic enables a more efficient placement of turbines in wind farms within the same land area.

2.Crucially, the J-shaped blade demonstrated a remarkable improvement in starting torque, achieving a torque that is 142% larger than that of the NACA0015 airfoil. This enhancement positions the turbine as a more viable and efficient solution for urban settings, addressing the challenges associated with initial rotation in low-wind conditions.

In summary, the integration of the proposed J-shaped blade not only maintains the overall performance of the Darrius turbine but also brings substantial advancements in starting torque, making it a promising innovation for urban wind energy applications. The research offers significant perspectives for the development and enhancement of Vertical-axis wind turbines. Paving the way for more sustainable and effective energy solutions in diverse environmental contexts.

References

according to
topics

(1) Zidane, Iham F, Khalid M Saqr, Greg Swadener, Xianghong Ma, and Mohamed F Shehadeh. "On the Role of Surface Roughness in the Aerodynamic Performance and Energy Conversion of Horizontal WindTurbine Blades: A Review." International journal of energy research 40, no. 15 (2016): 2054-77. https://doi.org/10.1002/er.3580
(2) Hau, Erich. Wind Turbines: Fundamentals, Technologies, Application, Economics. Springer Science & Business Media, 2013. https://doi.org/10.1007/978-3-642-27151-9
(3) Fischer, Gunter Reinald, Timoleon Kipouros, and Anthony Mark Savill. "Multi-Objective Optimisation of Horizontal Axis Wind Turbine Structure and Energy Production Using Aerofoil and Blade Properties as Design Variables." Renewable Energy 62 (2014): 506-15. https://doi.org/10.1016/j.renene.2013.08.009
(4) Bukala, Jakub, Krzysztof Damaziak, Krzysztof Kroszczynski, Marcin Krzeszowiec, and Jerzy Malachowski. "Investigation of Parameters Influencing the Efficiency of Small Wind Turbines." Journal of Wind Engineering and Industrial Aerodynamics 146 (2015): 29-38. https://doi.org/10.1016/j.jweia.2015.06.017
(5) Chen, Jian, Hongxing Yang, Mo Yang, and Hongtao Xu. "The Effect of the Opening Ratio and Location on the Performance of a Novel Vertical Axis Darrieus Turbine." Energy 89 (2015): 819-34. https://doi.org/10.1016/j.energy.2015.05.136
(6) Zamani, Mahdi, Mohammad Javad Maghrebi, and Seyed Rasoul Varedi. "Starting Torque Improvement Using J-Shaped Straight-Bladed Darrieus Vertical Axis Wind Turbine by Means of Numerical Simulation." Renewable Energy 95 (2016): 109-26. https://doi.org/10.1016/j.renene.2016.03.069

(7) Zamani, Mahdi, Saeed Nazari, Sajad A Moshizi, and Mohammad Javad Maghrebi. "Three Dimensional Simulation of J-Shaped Darrieus Vertical Axis Wind Turbine." Energy 116 (2016): 1243-55. https://doi.org/10.1016/j.energy.2016.10.031

(8) Mohamed, MH. "Criticism Study of J-Shaped Darrieus Wind Turbine: Performance Evaluation and Noise Generation Assessment." Energy 177 (2019): 367-85. https://doi.org/10.1016/j.energy.2019.04.102

(9) Rezaeiha, Abdolrahim, Hamid Montazeri, and Bert Blocken. "Towards Optimal Aerodynamic Design of Vertical Axis Wind Turbines: Impact of Solidity and Number of Blades." Energy 165 (2018): 1129-48. https://doi.org/10.1016/j.energy.2018.09.192

(10) Pan, Lin, Ze Zhu, Haodong Xiao, and Leichong Wang. "Numerical Analysis and Parameter Optimization of J-Shaped Blade on Offshore Vertical Axis Wind Turbine." Energies 14, no. 19 (2021): 6426. https://doi.org/10.3390/en14196426

(11) Daróczy, László, Gábor Janiga, Klaus Petrasch, Michael Webner, and Dominique Thévenin. "Comparative Analysis of Turbulence Models for the Aerodynamic Simulation of H-Darrieus Rotors." Energy 90 (2015): 680-90. https://doi.org/10.1016/j.energy.2015.07.102

(12) Zidane, Iham F, Khalid M Saqr, Greg Swadener, Xianghong Ma, and Mohamed F Shehadeh. "Computational Fluid Dynamics Study of Dusty Air Flow over Naca 63415 Airfoil for Wind Turbine Applications." Jurnal Teknologi 79, no. 7-3 (2017): 1-6. https://doi.org/10.11113/jt.v79.11877

(13) Zidane, IF, G Swadener, Khalid M Saqr, X Ma, and Mohamed F Shehadeh. "CFD Investigation of Transitional Separation Bubble Characteristics on Naca 63415 Airfoil at Low Reynolds Numbers." Paper presented at the Proceedings of the 25th UKACM Conference on Computational Mechanics, 2017.

(14) McLaren, K, S Tullis, and S Ziada. "Computational Fluid Dynamics Simulation of the Aerodynamics of a High Solidity, Small-Scale Vertical Axis Wind Turbine." Wind Energy 15, no. 3 (2012): 349-61. https://doi.org/10.1002/we.472

(15) Zhang, TT, Wei Huang, ZG Wang, and Li Yan. "A Study of Airfoil Parameterization, Modeling, and Optimization Based on the Computational Fluid Dynamics Method." Journal of Zhejiang University-SCIENCE A (Applied Physics & Engineering) 17, no. 8 (2016): 632-45. DOI:10.1631/jzus.A1500308

(16) Chen, Tao, and Tianshu Liu. "Lamb Dilatation and Its Hydrodynamic Viscous Flux in near-Wall Incompressible Flows." Physica D: Nonlinear Phenomena 448 (2023): 133730. https://doi.org/10.1016/j.physd.2023.133730

(17) Tatum, Jeremy. Classical Mechanics. LibreTexts, 2023.

(18) Trivellato, Filippo, and M Raciti Castelli. "On the Courant–Friedrichs–Lewy Criterion of Rotating Grids in 2d Vertical-Axis Wind Turbine Analysis." Renewable Energy 62 (2014): 53-62. https://doi.org/10.1016/j.renene.2013.06.022

(19) Lanzafame, Rosario, Stefano Mauro, and Michele Messina. "2d Cfd Modeling of H-Darrieus Wind Turbines Using a Transition Turbulence Model." Energy Procedia 45 (2014): 131-40. https://doi.org/10.1016/j.egypro.2014.01.015

(19) Lanzafame, Rosario, Stefano Mauro, and Michele Messina. "2d Cfd Modeling of H-Darrieus Wind Turbines Using a Transition Turbulence Model." Energy Procedia 45 (2014): 131-40. https://doi.org/10.1016/j.egypro.2014.01.015

(20) Langtry, Robin Blair. "A Correlation-Based Transition Model Using Local Variables for Unstructured Parallelized Cfd Codes." (2006). http://dx.doi.org/10.18419/opus-1705

(21) Ferreira, CJ Simao, GJW van Bussel, and GAM van Kuik. "2d Cfd Simulation of Dynamic Stall on a Vertical Axis Wind Turbine: Verification and Validation with Piv Measurements." Paper presented at the 45th AIAA Aerospace Sciences Meeting 2007, 8-11 January 2007, Reno, NV, 2007. 10.2514/6.2007-1367

(22) Maître, Thierry, Ervin Amet, and Christian Pellone. "Modeling of the Flow in a Darrieus Water Turbine: Wall Grid Refinement Analysis and Comparison with Experiments." Renewable Energy 51 (2013): 497-512. https://doi.org/10.1016/j.renene.2012.09.030

according to topics

(23) Bravo, R, S Tullis, and S Ziada. "Performance Testing of a Small Vertical-Axis Wind Turbine." Paper presented at the Proceedings of the 21st Canadian Congress of Applied Mechanics, 2007.

(24) Zidane, Iham F, Greg Swadener, Xianghong Ma, Mohamed F Shehadeh, Mahmoud H Salem, and Khalid M Saqr. "Performance of a Wind Turbine Blade in Sandstorms Using a Cfd-Bem Based Neural Network." Journal of Renewable and Sustainable Energy 12, no. 5 (2020) https://doi.org/10.1063/5.0012272

(25) Zidane, Iham F, Hesham M Ali, Greg Swadener, Yehia A Eldrainy, and Ali I Shehata. "Effect of Upstream Deflector Utilization on H-Darrieus Wind Turbine Performance: An Optimization Study." Alexandria Engineering Journal 63 (2023): 175-89. https://doi.org/10.1016/j.aej.2022.07.052

(26) Radhakrishnan, Jayakrishnan, Surya Sridhar, Mohammed Zuber, Eddie YK Ng, and Satish Shenoy. "Design optimization of a Contra-Rotating VAWT: A comprehensive study using Taguchi method and CFD." Energy Conversion and Management 298 (2023): 117766. https://doi.org/10.1016/j.enconman.2023.117766

(27) Afif, A. A., Putri Wulandari, and Ary Syahriar. "CFD analysis of vertical axis wind turbine using ansys fluent." In Journal of Physics: Conference Series, vol. 1517, no. 1, p. 012062. IOP Publishing, 2020. 10.1088/1742-6596/1517/1/012062

(28) Duty, Drusilla, Muhamad Johan, Yuwaraja Samy, Mohd Ezrin Indarah, Syahmi Shaharudin, Djamal Didane, and Bukhari Manshoor. 2023. “Performance Analysis of VAWT With H-Darrieus Rotor Using 2D CFD Modelling”. Journal of Design for Sustainable and Environment 5 (1), 5-10. https://www.jdse.fazpublishing.com/index.php/jdse/article/view/44.

Arab Academy

for Science , Technology and Maritime Transport

13 Marlog 2024

The International Maritime Transport and Logistics Conference

"MARLOG 13"

Thank You